

# The Proteolytically Stable Peptidomimetic Pam-(Lys-ßNSpe)6-NH2 Selectively Inhibits Human Neutrophil Activation via Formyl Peptide Receptor 2

**Skovbakke, Sarah Line; Heegaard, Peter M. H.; Larsen, Camilla J.; Franzyk, Henrik; Forsman, Huamei; Dahlgren, Claes**

*Published in:*
Biochemical Pharmacology

*Link to article, DOI:*
10.1016/j.bcp.2014.11.004

*Publication date:*
2015


Title: The Proteolytically Stable Peptidomimetic Pam-(Lys-βNSpe)$_6$-NH$_2$ Selectively Inhibits Human Neutrophil Activation via Formyl Peptide Receptor 2

Author: Sarah Line Skovbakke Peter M.H. Heegaard Camilla J. Larsen Henrik Franzyk Huamei Forsman Claes Dahlgren

PII: S0006-2952(14)00661-3
DOI: http://dx.doi.org/doi:10.1016/j.bcp.2014.11.004
Reference: BCP 12135

To appear in: *BCP*

Received date: 23-9-2014
Revised date: 7-11-2014
Accepted date: 7-11-2014

Please cite this article as: Skovbakke SL, Heegaard PMH, Larsen CJ, Franzyk H, Forsman H, Dahlgren C, The Proteolytically Stable Peptidomimetic Pam-(Lys-*rmbeta*NSpe)$_6$-NH$_2$ Selectively Inhibits Human Neutrophil Activation via Formyl Peptide Receptor 2, *Biochemical Pharmacology* (2014), http://dx.doi.org/10.1016/j.bcp.2014.11.004

# *The Proteolytically Stable Peptidomimetic Pam-(Lys-βNSpe)$_6$-NH$_2$ Selectively Inhibits Human Neutrophil Activation via Formyl Peptide Receptor 2*

**Sarah Line Skovbakke[a,b], Peter M. H. Heegaard[c], Camilla J. Larsen[a], Henrik Franzyk[a], Huamei Forsman[b], Claes Dahlgren[b]**

[a] Department of Drug Design and Pharmacology, Faculty of Health and Medical Sciences, University of Copenhagen, Universitetsparken 2, DK-2100 Copenhagen, Denmark.
S. L. S. email: sals@sund.ku.dk, C. J. L. email: Camilla.josephine.larsen@gmail.com, H.F. email: henrik.franzyk@sund.ku.dk

[b] Department of Rheumatology and Inflammation Research, Institute of Medicine, Sahlgrenska Academy, University of Gothenburg, Guldhedsgatan 10A, 413 46 Gothenburg, Sweden.
H.F. email: Huamei.forsman@rheuma.gu.se, C. D. email: claes.dahlgren@rheuma.gu.se

[c] Innate Immunology Group, National Veterinary Institute, Technical University of Denmark, Copenhagen, Denmark, Bülowsvej 27, DK-1870 Frederiksberg C, Denmark.
P.M.H.H. email: PMHH@vet.dtu.dk

Corresponding author: S. L. Skovbakke, Address: Department of Drug Design and Pharmacology, Faculty of Health and Medical Sciences, University of Copenhagen, Universitetsparken 2, DK-2100, Copenhagen, Denmark, e-mail: sals@sund.ku.dk, telephone: +45 35336336

**Category:** Inflammation and Immunopharmacology

## *List of abbreviations*

2-Aoc, 2-aminooctanoic acid; Ac, acetyl; AMP, antimicrobial peptide; βNphe, *N*-phenyl-β-alanine; βNSpe, *N*-(*S*)-1-phenylethyl-β-alanine; C5a, complement fragment 5a; C5aR, receptor for C5a; $[Ca^{2+}]_i$, concentration of free intracellular calcium; CF, carboxyfluorescein; CL, chemiluminescense; Cmp. 43, compound 43 (FPR1 ligand); CsH, cyclosporine H; CXCR, CXC chemokine receptor; DAD, diode array detector; DMF, Dimethylformamide; ESI-MS, electrospray ionization mass spectrometry; DIPEA, diisopropylethylamine; FCS, fetal calf serum; F2Pal10, FPR2-derived pepducin; FPR, formyl peptide receptor; GPCR, G-protein coupled receptor; hArg, homoarginine; HDP, host defense peptide; HPLC, high-performance liquid chromatography; HRP, horseradish peroxidase; HR-MS, High-resolution mass spectrometry; IDR, innate defense regulator; KRG, Krebs-Ringer phosphate buffer with glucose; Lau, lauryl; Lys, lysine; Lys(Pam); $N^{\varepsilon}$-palmitoyl-lysine; mAb, monoclonal antibody; Me, methyl; NLys, α-peptoid lysine; Oct, octanoyl; OSu, *N*-hydroxysuccinimidyl; PAF, platelet-activating factor; PAFR, receptor for PAF; Pam, palmitoyl; PBP10, Rhodamine-B labelled Phosphatidylinositol 4,5-bisphosphate-binding peptide derived from gelsolin; PE, phycoerythrin; PFA, paraformaldehyde; Ph, phenyl; PLC, phospholipase C; PMA, phorbol myristate acetate, PMN, polymorphonuclear leukocytes; PRR, pattern recognition receptor; PSM, phenol-soluble modulin; PyBOP, (benzotriazol-1-yloxy)-tris(pyrrolidino)phosphonium hexafluorophosphate; ROS, reactive oxygen species; RPMI, RPMI-1640 culture medium; SOD, superoxide dismutase; Ste, steroyl; TFA, trifluoroacetic acid

## *Abstract*

Immunomodulatory host defense peptides (HDPs) are considered to be lead compounds for novel anti-sepsis and anti-inflammatory agents. However, development of drugs based on HDPs has been hampered by problems with toxicity and low bioavailability due to *in vivo* proteolysis. Here, a subclass of proteolytically stable HDP mimics consisting of lipidated α-peptide/β-peptoid oligomers was investigated for their effect on neutrophil function. The most promising compound, Pam-(Lys-βNSpe)$_6$-$NH_2$, was shown to inhibit formyl peptide receptor 2 (FPR2) agonist-induced neutrophil granule mobilization and release of reactive oxygen species. The potency of Pam-(Lys-βNSpe)$_6$-$NH_2$ was comparable to that of PBP10, the most potent FPR2-selective inhibitor known. The immunomodulatory effects of structural analogues of Pam-(Lys-βNSpe)$_6$-$NH_2$ emphasized the importance of both the lipid and peptidomimetic parts. By using imaging flow cytometry in primary neutrophils and FPR-transfected cell lines we found that a fluorescently labelled analogue of Pam-(Lys-βNSpe)$_6$-$NH_2$ interacted selectively with FPR2. Furthermore the interaction between Pam-(Lys-βNSpe)$_6$-$NH_2$ and FPR2 was found to prevent binding of the FPR2-specific activating peptide agonist Cy5-WKYMWM, while the binding of a FPR1-selective agonist was not inhibited. To our knowledge, Pam-(Lys-βNSpe)$_6$-$NH_2$ is the first HDP mimic found to inhibit activation of human neutrophils via direct interaction with FPR2. Hence, we consider Pam-(Lys-βNSpe)$_6$-$NH_2$ to be a convenient tool in the further dissection of the role of FPR2 in inflammation and homeostasis as well as for investigation of the importance of neutrophil stimulation in anti-infective therapy involving HDPs.

**Keywords:** Formyl peptide receptors, neutrophils, anti-inflammatory, host defense peptides, G-protein coupled receptors

## *1. Introduction*

The innate immune response constitutes the front-line defense against infection [1]. It consists of a complex network of cells and inducible soluble factors that interact to recognize and combat incoming pathogens in a series of immediate and relatively unspecific and generalized reactions. Microbial molecular components are recognized via pattern recognition receptors (PRRs) on host immune cells resulting in the release of pro-inflammatory and antibacterial factors such as cytokines, chemokines, lipid mediators, and reactive oxygen species (ROS) [2]. Local inflammation plays an important role in this response by orchestrating the recruitment of various immune cells to the infection focus often resulting in clearance of the infection. However, excessive, unbalanced, or prolonged inflammation can be detrimental to the host. In the case of sepsis, the massive release of pro-inflammatory factors into the circulation causes tissue damage possibly leading to organ dysfunction and ultimately death [3-5]. Novel anti-infective therapies are urgently needed due to the fact that excessive and non-compliant use of antibiotics has selected for multidrug-resistant bacterial strains. Consequently, infectious diseases are once again becoming a severe health threat as we are rapidly approaching what has been termed "the post-antibiotic era" [6-8]. As the innate immune response is involved in the initial protection against invasive microorganisms as well as in the pathogenesis of infectious and inflammatory diseases, immunomodulation has been proposed as an attractive novel non-antibiotic therapeutic approach [9, 10]. Natural host defense peptides (HDPs) possess many of the properties essential for anti-infective agents as

a number of these peptides exhibit both direct microbicidal activity and potent immunomodulatory functions via interaction with various immune-competent cells such as neutrophils [10-12]. Being among the first cells to be recruited to the site of infection, neutrophils are important early effector cells of the innate immune system. Moreover, dysregulation of neutrophil function has been linked to both aseptic and septic inflammatory and autoimmune diseases, highlighting the importance of this cell type in maintaining a balanced inflammatory response [13-18]. Recruitment and activation of neutrophils occur through integration of signals from cell-surface G-protein coupled receptors (GPCRs) recognizing host factors such as chemotactic proteins and peptides, e.g. chemokines via CXCR1/2, and complement anaphylatoxins via C5aR, as well as pathogen-derived N-formylated peptides via formyl peptide receptors (FPRs) [2, 19]. Human neutrophils express two closely related FPRs, namely FPR1 and FPR2 [20]. Activation of neutrophils through FPRs induces a variety of pro-inflammatory and antibacterial effector mechanisms including production of ROS, and release of antimicrobial peptides (AMPs) and hydrolytic enzymes from intracellular granules [20]. Furthermore, FPRs regulate the inflammatory reactions in neutrophils by modulating signaling through many other receptors in a process termed receptor cross-talk [21-24]. The role of FPRs in regulation of inflammation is highlighted by their suggested involvement in both systemic [25] and local [26-28] inflammatory responses. Thus, recently various groups have suggested FPRs as therapeutic targets in inflammatory and infectious diseases [29, 30] and several selective FPR agonists and inhibitors have been discovered: the cyclic undecapeptide cyclosporine H (CsH) is the most potent selective FPR1 inhibitor [31, 32], and rhodamine B-labelled $PIP_2$-binding peptide of gelsolin (PBP10) is the most potent selective FPR2 inhibitor known to date [33, 34]. Also several HDPs have been shown to interact with FPRs thereby modulating the responses of human neutrophils [35-40],

e.g. human cathelicidin LL-37, a chemoattractant that activates neutrophils through FPR2 [36, 37, 39, 40]. Furthermore, a synthetic derivative of bactenecin (a bovine HDP), referred to as innate defense regulator peptide 1 (IDR-1), has been shown to induce neutrophil migration and activation thereby augmenting neutrophil-mediated killing of bacteria via FPR1 [41]. Development of anti-infective drugs based on HDPs has been hampered by problems with toxicity and poor bioavailability due to *in vivo* proteolytic degradation [42]. To circumvent these problems, we and others have developed synthetic HDP mimics with improved characteristics such as increased protease resistance [43-45]. Stable HDP mimics based on a design with alternating α-amino acids and peptoid residues (see Figure 1A) have been found to exhibit antimicrobial activity against planktonic bacteria and biofilm, and to possess antiplasmodial as well as immunomodulatory activities [43, 46-49]. The aim of the present study was to investigate the effects of lipidated peptidomimetics, belonging to the subclass of α-peptide/β-peptoid hybrids, on the inflammatory responses of human neutrophils. The most promising compound, Pam-(Lys-βNSpe)$_6$-$NH_2$ (Cmp. **1**, Figure 1B), displayed receptor-selective inhibition of cellular responses, such as production of ROS and degranulation induced in neutrophils by FPR2-specific agonists, with a potency comparable to that of the most potent known FPR2 inhibitor PBP10. Based on these results Pam-(Lys-βNSpe)$_6$-$NH_2$ is considered to be a promising anti-inflammatory drug lead that may prove useful for the treatment of inflammation-driven disease, including sepsis. Furthermore, Pam-(Lys-βNSpe)$_6$-$NH_2$ may be a useful tool in the further dissection of the role of FPR2 in inflammation and homeostasis.

## *2. Materials and Methods*

### *2.1 Chemicals, reagents and peptides*

Solvents, Rink amide resin, α-amino acid building blocks and coupling reagents were obtained from IrisBiotech (Marktredwitz, Germany), while octanoic acid, Lau-OSu and Pam-OSu, stearic acid, and 5(6)-carboxyfluorescein (CF) were obtained from Sigma-Aldrich Chemie (Steinheim, Germany); Fmoc-Lys(Pam)-OH was acquired from Bachem (Bubendorf, Switzerland). Horseradish peroxidase (HRP) and phorbol myristate acetate (PMA) were from Sigma-Aldrich (St. Louis, MO, USA). PBP10 peptide (RhB-QRLFQVKGRR) and the FPR2-derived pepducin F2Pal10 (palmitoyl (Pam)-KIHKKGMIKS) were obtained from Caslo Laboratory (Lyngby, Denmark). The receptor antagonist WRWWWW (WRW4) was from Genscript Corporation (Scotch Plains, NJ, USA) and cyclosporin H was kindly provided by Novartis Pharma (Basel, Switzerland). The hexapeptides WKYMWM/m were purchased from AltaBioscience (University of Birmingham, Birmingham, U.K.), and the phenol-soluble modulin (PSMα2, MGIIAGIIKFIKGLIEKFTGK) was obtained in its α-N-formylated form from American Peptide Company (Sunnyvale, CA, USA). The formylated tripeptide fMLF and C5a were purchased from Sigma-Aldrich (St. Louis, MO) and PAF was from Avanti Polar Lipids Inc. (Alabama, USA). The FITC-fNLFNYK and the Cy5-WKYMWM peptides were from Phoenix Pharmaceutical (Burlingame, CA). All peptides were dissolved in dimethyl sulfoxide to a concentration of 10 mM and stored at –80°C until use. Further dilutions were made in Krebs-Ringer phosphate buffer that was supplemented with glucose

(10 mM), $Ca^{2+}$ (1 mM), and $Mg^{2+}$ (1.5 mM) (KRG; pH 7.3). RPMI 1640, fetal calf serum (FCS), penicillin and streptomycin, and G418 were from PAA Laboratories GmbH, Austria.

*2.2 General procedure for purification and compound characterization*

Analytical HPLC was performed on a Shimadzu HPLC system with diode array detector (DAD) consisting of an SCL-10A VP controller, an SIL-10AD VP auto injector, an LC-10AT VP Pump, an SPDM10A VP DAD, and a CTO-10AC VP column oven, using a Phenomenex Luna C18(2) column (150 × 4.6 mm ; 3 μm) eluted at a rate of 0.8 mL/min. Injection volumes were 5-10 μL of a 1 mg/mL solution and separations were performed at 40 °C. The system was controlled by Class VP 6 software. Eluents A ($H_2O$/MeCN/TFA) 95:5:0.1) and B (MeCN/$H_2O$/TFA 95:5:0.1) were employed for linear gradient elution (10% B → 60% B during 30 min or 20% B → 100% B during 30 min). Preparative HPLC separations were performed on a Phenomenex Luna C18(2) column (250 × 21.2 mm; particle size: 5 μm) by using an Agilent 1100 system consisting of two preparative-scale pumps, an autosampler, and a multiple-wavelength UV detector. The eluents A and B were employed with a flow rate of 20 mL/min; injection volumes were 300-900 μL; typically, linear gradients of 10% B → 60% B during 20 min or 20% B → 80% B during 20 min were employed. High-resolution mass spectra were obtained on a Bruker MicroTOF-Q LC mass spectrometer equipped with an electrospray ionization source and a Quadropole MS detector. The analyses were performed as ESI-MS (m/z): $[M + nH]^{n+}$ for all peptidomimetics.

*2.3 Synthesis of peptidomimetics*

The α-peptide/β-peptoid peptidomimetics **1-16**, peptides **17** and **18** as well as peptoid **19-21** (Figure 1) were synthesized on Rink amide resin by standard Fmoc solid-phase synthesis using the appropriate dimeric building blocks [50] and peptoid lysine building block [46, 51] with PyBOP as coupling reagent as earlier reported [50]. In the lipidated compounds the acyl moieties were introduced either via coupling of the corresponding acid (5 equiv, 16 h; octanoic acid, stearic acid, or commercial Fmoc-Lys(Pam)-OH) using PyBOP (5 equiv) as coupling reagent (in DMF; 10 equiv DIPEA) or via the N-hydroxysuccinimidyl esters (Lau-OSu and Pam-OSu in DMF; equiv DIPEA, 16 h). The fluorophore in compounds **20** and **21** was introduced as earlier described [48]. Following cleavage from the resin, all peptidomimetics were purified to homogeneity by preparative HPLC. The identity of the compounds was verified by HR-MS ($\Delta M < 5$ ppm), and the purity was determined by using analytical HPLC (> 95% at 220 nm). Target compounds were stored dry at −20 °C until use.

*2.4 Isolation of human neutrophils*

Human polymorphonuclear neutrophils (PMNs) were isolated from buffy coats (The Blood Center, Sahlgrenska University Hospital, Gothenburg) obtained from apparently healthy adults. After storage overnight at ambient temperature erythrocytes were depleted by dextran sedimentation at 1 × g and the leukocyte mixture was centrifuged on a Ficoll-Paque gradient. After a hypotonic lysis of the remaining erythrocytes, the PMNs were washed twice, resuspended ($1 \times 10^7$/mL) in KRG, and kept on melting ice until use.

*2.5 Expression of FPRs in undifferentiated HL60 cells*

The stable expression of FPR1 and FPR2 in undifferentiated HL60 cells has been described previously [31, 52, 53]. To prevent auto-differentiation, cells were passed twice a week before reaching a density of $2 \times 10^6$/ml. At each passage, an aliquot of cells was centrifuged, the supernatant discarded, and the cell pellet resuspended in fresh culture medium containing RPMI 1640 supplemented with FCS (10%), penicillin/streptomycin (1%), L-glutamine (2 mM) and the selection antibiotic G418 (1 mg/mL).

*2.6 Neutrophil NADPH-oxidase activity*

Superoxide anion production was determined by using luminol- or isoluminol-enhanced chemiluminescense (CL) systems [54, 55]. The CL activity was measured in a 6-channel Biolumat LB 9505 (Berthold Co, Wildbad, Germany) using disposable 4-mL polypropylene tubes with a 1 mL reaction mixture. The release of ROS was measured with cells in KRG (PMNs or differentiated HL60 cells at a density of $2 \times 10^5$/mL) mixed with isoluminol ($2 \times 10^{-5}$ M) and HRP (4 U/mL). The cells were pre-warmed for 5 min at 37$^o$C in the presence or absence of receptor inhibitors, after which the stimulus was added. The light emission was recorded continuously for up to 20 min.

*2.7 Changes in the intracellular concentration of $Ca^{2+}$*

Freshly isolated PMNs from buffy coats or undifferentiated stably transfected HL60 cells ($2 \times 10^7$/mL) were labeled with Fura 2-AM (Molecular Probes, Eugene, OR, USA), and the change in the cytosolic concentration $Ca^{2+}$ was followed by the use of a PerkinElmer fluorescence spectrophotometer (LC50) as previously described [52]. The transient rise in

intracellular calcium is presented as the ratio between fluorescence intensities of the emitted light at 340 nm and 380 nm when excited at 510nm.

*2.8 Cell-surface receptor expression*

The level of surface expression of the integrin CR3 was determined by the use of a phycoerythrin (PE)-conjugated antibody against CD11b (BD Biosciences, MD, USA). To surface label the PMNs, cells in KRG ($5 \times 10^6$/mL) were incubated on ice, the antibodies were added and the incubation was prolonged for 30 min. Control samples incubated with isotype control antibodies were included. After a washing step to remove excess unbound antibodies, the amount of bound fluorescence was determined by flow cytometry using an Accuri C6 flow cytometer (Becton Dickinson Sparks, MD, USA). Surface expression of FPR2 was determined using an FPR2-specific mAb (Abcam, Cambridge, UK) together with a goat anti-mouse IgG secondary antibody (Thermo Scientific, Waltham, MA, USA). PMNs ($1 \times 10^6$/mL) suspended in ice cold PBS supplemented with 1% BSA were incubated with the anti-FPR2 mAb on ice for 30 min. Control samples incubated with an isotype control were included. After washing, the cells were incubated with the secondary antibody for 20 min on ice. After a final wash the cells were fixed by incubation in 2% PFA for 10 min at room temperature, washed in PBS/BSA, and kept cold until analysis.

*2.9 Evaluation of ligand-receptor interaction by imaging flow cytometry*

Primary human neutrophils, or HL60 cells stably transfected with either FPR1 or FPR2, were stained with the CF-labelled compounds **20** and **21** (Figure 1), or an FPR2-specific mAb/secondary antibody pair (see below) before analysis by imaging flow cytometry

(ImageStream X, see below). The staining with CF-labelled compounds was performed by adding a final concentration of 100 nM compound **20** or **21** to cells in ice cold KRG ($1 \times 10^6$ cells/mL) followed by incubation on ice for 30 min. The cells were fixed immediately hereafter by addition of 2% PFA, and incubation for 10 min at room temperature. After fixation the cells were washed once, resuspended in KRG, and kept cold until analysis. Staining of the nucleus with DRAQ5 (Abcam, Cambridge, UK) was performed immediately before analysis by addition of DRAQ5 (5 μM) to each sample followed by incubation for 5 min at room temperature. Staining of separate cell samples for FPR2 expression was performed as described above for flow cytometry. For each sample 5000 focused cells were collected using an ImageStream X (Amnis, Seattle, WA, USA) imaging flow cytometer with 60x objective without extended depth of field. IDEAS® software v. 6.0 (Amnis, Seattle, WA, USA) was used for data analysis (additional information about the used features and calculations performed can be found in the IDEAS® user manual that may be downloaded from www.amnis.com). First, cells in focus were gated, followed by identification of single cells in a plot of Aspect Ratio (the length of the minor axis of an object divided by the length of the major axis) versus Area in the Brightfield channel, and analysis of fluorescence intensity and distribution. The cellular distribution of fluorescence was analyzed using the Bright Detail Intensity R3 feature of the IDEAS software. Bright Detail Intensity R3 computes the fluorescence intensity in bright spots of 3 pixels or less in the cell after subtraction of the local background surrounding the spots.

*2.10 Competitive receptor binding by flow cytometry*

Neutrophils in ice cold KRG ($5 \times 10^6$/mL) were preincubated with unlabeled ligands or inhibitors for 5 min on ice before addition of fluorescently labeled FPR2-specific (Cy5-WKYMWM) or FPR1-specific (FITC-fNLFNYK) agonist followed by incubation on ice for 30 min. The neutrophils were fixed directly after labeling by addition of 2% PFA and incubated at room temperature for 10 min. After fixation the cells were washed once, resuspended in KRG, and kept cold until analysis by flow cytometry using an Accuri C6 flow cytometer (Becton Dickinson Sparks, MD, USA).

*2.11 Statistical analysis*

All statistical analyses were performed using GraphPad Prism 6.0. Statistical comparison of different treatments was performed by one- or two-way ANOVA followed by the recommended adjustment for multiple comparisons as indicated for specific experiments; $p < 0.05$ was considered statistically significant. $IC_{50}$-values for selective receptor inhibitors and α-peptide/β-peptoid chimeric oligomers were determined by fitting a sigmoidal curve with variable slope to data normalized to the response induced without inhibitors (= 100%) using the "log(inhibitor) versus normalized response" function in GraphPad Prism. A "Replicates Test for Lack of Fit" was performed and showed no evidence for use of an inadequate model.

## *3. Results*

Modulation of inflammatory cell functions constitutes a novel promising approach that on one hand may target bacterial infections and on the other hand may prevent or cure excessive inflammatory responses leading to disease [9-11]. Inspired by our previous finding that an α-peptide/α-peptoid hybrid exhibited moderate immunomodulatory activity [48], we screened an array of analogous α-peptide/β-peptoid oligomers (see Figure 1A) with different N-terminal modifications for their ability to inhibit release of pro-inflammatory cytokines from stimulated leukocytes. The lipidated peptidomimetic Pam-(Lys-βNSpe)$_6$-$NH_2$ (compound **1**, see Figure 1B) was identified as having potent anti-inflammatory properties (submitted for publication). In the present study, the effect of compound **1** on inflammatory responses of neutrophils was investigated.

### *3.1 Modulation of FPR2 mediated superoxide release and degranulation by Pam-(Lys-βNSpe)$_6$-$NH_2$ (compound **1**)*

Initially we investigated the ability of compound **1** to modulate superoxide release upon triggering of neutrophils with receptor-specific chemoattractants or the receptor-independent phospholipase C (PKC) activator phorbol myristate acetate (PMA). The neutrophils were pre-incubated with the compound (0.5 – 1.0 μM) for a short time (5 min) and then stimulated with receptor-specific agonists known to induce an activation of the superoxide-generating NADPH-oxidase. The selective agonists comprise the complement protein fragment C5a

(agonist of the C5a-receptor, C5aR), platelet-activating factor (PAF; agonist of the PAF-receptor, PAFR), as well as the two peptides fMLF, and WKYMWM, selective for FPR1 and FPR2, respectively. The response induced by the FPR2 agonist WKYMWM was inhibited significantly whereas compound **1** had no effect on the responses induced by the other stimuli (data for the two FPR agonist and PMA are shown in Figure 2A. Data for different concentrations of compound **1** are shown in Figure 5A.). FPR2 unresponsiveness can be induced through binding of specific FPR agonists after a short period of active signaling in a process called homologous desensitization [56-58]. Consequently, we wished to investigate whether compound **1** activates neutrophil production of superoxide anions and desensitizes the cells for a challenge with a new receptor agonist but no such effect was seen. In concentrations that completely inhibit the activity induced by WKYMWM (0.5 - 1.0 μM), no direct activation was induced by compound **1**, as no release of ROS or any intracellular ROS production was seen in neutrophils (data not shown). Binding of chemoattractants to their respective neutrophil GPCRs not only induces activation of the NADPH-oxidase, but also triggers mobilization of receptors localized in granule/secretory vesicle compartments to the plasma membrane [19]. Accordingly, activation of neutrophils by FPR agonists results in the mobilization of CD11b (CR3) to the cell surface, as shown in Figure 2B for the FPR1 agonist fMLF and the FPR2 agonist WKYMWM. In accordance with the results obtained in the NADPH-oxidase assay, addition of submicromolar concentrations of compound **1** selectively inhibited the WKYMWM-induced CD11b mobilization by more than 50%, similarly to the well-established FPR2 inhibitor PBP10, whereas the fMLF response was unaffected (see Figure 2B). FPR2 is a promiscuous receptor, and some of the known agonists also activate FPR1. To determine whether the inhibitory activity of compound **1** is ligand- or receptor-dependent, several previously characterized FPR ligands (peptides and lipopeptides)

possessing somewhat different selectivity or mode of action were used to determine the inhibitory effects of compound **1** (see Figure 3A and B). The response induced by the agonists fMLF and compound 43 (Cmp. 43), that both prefer FPR1 over FPR2, was not inhibited by compound **1** (0.5 μM). The hexapeptide WKYMVm is an agonist that activates both neutrophil FPRs and in accordance with this the NADPH-oxidase activity induced by this dual agonist was not affected significantly by neither compound **1** (0.5 μM) nor CsH (1.0 μM) when added separately. Combining compound **1** with CsH, on the other hand, inhibited the response to WKYMWm, as would be expected if compound **1** is a selective FPR2 inhibitor. In accordance with the suggested FPR2 selectivity of compound **1** (0.5 μM), it completely inhibited the responses induced by the FPR2-selective peptide agonists WKYMWM and MMK1 [59] as well as by the staphylococcal phenol-soluble modulin (PSMα2) [60] (Figure 3A). It is well-known that several GPCRs may be activated by a group of lipopeptides classified as pepducins [61, 62]. A typical pepducin contains a palmitic acid residue linked to a peptide with a sequence corresponding to an intracellular segment of the corresponding GPCR. The most potent pepducin derived from the third intracellular loop of FPR2, denoted F2Pal10, was recently shown to selectively activate neutrophils via FPR2 [62]. The inhibitory effect of compound **1** (0.5 μM) was not restricted to conventional FPR2 agonists, but also included suppression of the response induced by the pepducin F2Pal10 (see Figure 3B).

*3.2 Compound **1** inhibits FPR2-induced increase in free cytosolic $Ca^{2+}$-concentration*

A very early event in signaling upon activation of FPRs is a phospholipase C-dependent increase in the cytosolic $Ca^{2+}$-concentration ($[Ca^{2+}]_i$), a rise initially achieved via mobilization of $Ca^{2+}$ from intracellular storage organelles [33]. Although this signaling pathway is not

directly linked to that leading to an activation of the NADPH-oxidase [56] we used this secondary messenger to determine whether the effect of compound **1** on activation through FPR2 is due to interference with the early part of the signaling cascade, rather than blocking the receptor itself. Compound **1** (1.0 μM) selectively and dose-dependently inhibited the rise in $[Ca^{2+}]_i$ induced by the FPR2-specific agonist WKYMWM, whereas $Ca^{2+}$ mobilization triggered by the FPR1-specific agonist fMLF was unaffected (see Figure 4, part A and B). The FPR2 selectivity of compound **1** was also confirmed by experiments performed on stably transfected HL60 cells expressing either FPR1 or FPR2 [52]. The functionality and selective expression of FPRs in these cells were verified by the inhibitory effects on the changes of $[Ca^{2+}]_i$ in the presence of the earlier described receptor-selective inhibitors CsH and PBP10 (Figure 4C). The FPR1-specific antagonist CsH (1.0 μM) inhibited the fMLF induced response as expected, while PBP10 (1.0 μM) was without effect on the rise in $[Ca^{2+}]_i$ in FPR1-expressing cells activated with fMLF, and this was found to be the case also for compound **1** (1.0 μM). In accordance with the FPR2 selectivity of compound **1** (1.0 μM) and PBP10 (1.0 μM) both efficiently inhibited the response induced by WKYMWM in FPR2-transfected cells, whereas the FPR1-selective inhibitor CsH (1.0 μM) was without effect (Figure 4C). In summary, these results clearly demonstrate that compound **1** affects early events of FPR2 signaling and that the presence of FPR2 is required for its activity.

*3.3 Potency and activity of compound **1** is similar to that of PBP10*

Previous studies have identified two selective inhibitors of FPR2, namely the classical peptide antagonist $WRW_4$ and the allosteric modulator PBP10 [33, 53, 63, 64]. Comparison of the inhibitory efficiency of compound **1** with these known FPR2 inhibitors was performed on the

WKYMWM-induced NADPH-oxidase response in human neutrophils. This revealed similar inhibitory profiles for compound **1** and PBP10, with an $IC_{50}$ value of compound **1** slightly lower than that for PBP10 (50 nM vs. 60 nM; Figure 5A). Compared to the antagonist $WRW_4$, both compound **1** and PBP10 were significantly more potent (see Figure 5A). To investigate the apparent similarity in effect and mode of action of compound **1** and PBP10 further, the combined effect of lower concentrations (0.05 μM) of the two inhibitors was determined. As seen in Figure 5B, a purely additive effect of the two inhibitors was found. In addition, the reversibility of their effects was investigated. Neutrophils ($2\times10^7$ cells/mL) were preincubated with inhibitory concentrations (0.2 μM) of either compound **1** or PBP10 for 2 min. The cell suspensions were diluted 100-fold, giving a non-inhibitory concentration of the inhibitors (0.002 μM), and after various time periods of recovery the cells were subjected to stimulation with the FPR2-selective peptide WKYMVM in the presence (dashed line) or absence (dotted line) of freshly added inhibitor (0.2 μM). Already after 1 min of recovery after dilution, the cells without addition of more inhibitor (dotted line) were fully responsive to WKYMVM (Figure 5; shown for compound **1** in the left panel, and for PBP10 in the right panel), suggesting a rapid and fully reversible inhibition, and thus that persistent interaction with the receptor is required for inhibition.

*3.4 Structural determinants for the FPR2-inhibitory potency of compound **1***

To gain more insight into the structural requirements for the novel type of peptidomimetic FPR2 inhibitor, we investigated the structure-activity relationships within an array of diverse representatives of lipidated α-peptide/β-peptoid hybrid oligomers. Thus, a library of structural analogues of compound **1** was designed and synthesized (structures are presented in Figure

1B) and tested for their effects on FPR1- and FPR2-induced NADPH-oxidase activity. A non-lipidated derivative (compound **2**) showed no inhibitory activity in the concentration range tested (up to 1.0 μM), while analogues with gradually shorter lipid anchors (i.e. **4** and **5**) were less potent with rapidly increasing $IC_{50}$ values (Table 1), indicating that hydrophobicity is an important determinant for activity. However, compound **3**, containing a fatty acid that is longer than that of compound **1**, was only slightly more potent. Interestingly, overall hydrophobicity is not the parameter that alone determines the FPR2 inhibition potency. This conclusion was drawn from the fact that the variant in which the palmitoyl group was replaced by two shorter fatty acids (compound **6;** having the same hydrophobicity score as compound **1**) was a less efficient inhibitor than compound **1**. Alternatively, hydrophobicity may be introduced via incorporation of a synthetic α-amino acid displaying a $C_6$ side chain (i.e. 2-aminooctanoic acid: 2-Aoc) as the N-terminal residue(s). The FPR2 inhibitory effect of compound **7**, containing one N-terminal 2-Aoc residue, was comparable to that of compound **5** displaying an N-terminal octanoyl moiety. By contrast, incorporating two consecutive 2-Aoc residues (i.e. compound **8**) was less efficient than an N-terminal conjugation with a single $C_{12}$ fatty acid (i.e. compound **4**) supporting the hypothesis that hydrophobicity preferably should be present as a single long lipid chain in order to confer optimal FPR2 inhibitory function to these lipidated peptidomimetics. Additionally, the alternating cationic/hydrophobic design of the α-peptide/β-peptoid oligomers was found to be of importance since no inhibitory activity was obtained with the purely cationic lipidated compounds **17**-**19**. Variation in the type of cationic residues (i.e. compound **1** vs. **10**) and degree of chirality (i.e. compound **1** vs. **9**) only gave rise to minor differences in potency. Importantly, we found that full or partial exchange of the cationic lysine residues in compound **1** for the guanidinylated homoarginine (hArg; i.e. compound **10** and **13,**

respectively) resulted in loss of selectivity for FPR2, as the fMLF-induced release of ROS also was inhibited by compounds containing hArg residues (Table 1). Also, the length of the α-peptide/β-peptoid oligomer was found to be of some importance. Decreasing the length of the peptidomimetic moiety from twelve residues (as in compound **1** and **13**) to four residues (i.e. compound **11**) significantly decreased the FPR2-inhibitory effect. Interestingly, a non-lipidated 16-mer compound (i.e. compound **15**) was found to possess a surprisingly high FPR2-inhibitory activity albeit still 10-fold lower than the best lipidated oligomers. In summary, these data show that the FPR2-inhibitory activity of lipidated α-peptide/β-peptoid hybrid oligomers is dependent on the type of fatty acid as well as the design and length of the peptidomimetic oligomer. Furthermore, the FPR2 selectivity is dependent on the type of cationic residues used in the oligomers since compounds that only contain guadinylated cationic residues also inhibit FPR1.

*3.5 Interaction of lipidated α-peptide/β-peptoid hybrids with FPR2 prevent binding of WKYMWM*

Imaging flow cytometry was applied to investigate the interaction of a fluorescently labeled analogue of compound **1** with neutrophils. The CF-labeled analogue (i.e. compound **20** Figure 1B) retained an FPR2-selective inhibitory profile (0.05 - 0.5 μM), whereas the fluorescently labeled non-lipidated variant (compound **21**) displayed no inhibitory effect in the concentrations used (Figure 6A), in line with the activity of the lipidated versus the non-lipidated analogues (Table 1). Although neutrophils incubated with compound **21** (0.1 μM) showed some fluorescence, this was significantly lower (Figure 6B-C) compared to that observed for compound **20**. The images furthermore show that compound **20** is localized

primarily at the cell surface, whereas the non-lipidated (and non-inhibitory) compound **21** is distributed homogenously in the cytoplasm. The inferred difference in cellular distribution was verified by using image analysis to calculate the feature 'bright-detail intensity' (see section 2.9) of the cells incubated with compounds **20** and **21**, respectively (Figure 6D). We hypothesized that direct interaction of compound **20** (but not of **21**) with FPR2 might be the cause of the difference in cellular distribution between the two compounds. To probe this hypothesis, the cellular distribution of compounds **20** and **21** in HL60 cells, overexpressing either FPR1 or FPR2, was investigated. A clear difference in the cellular distribution of the active FPR2 inhibitor compound **20** (0.1 μM) in the two cell lines was observed (Figure 7A and B). In the FPR2-expressing cells compound **20** was localized primarily at the cell surface whereas it was distributed in the cytoplasm of the FPR1-expressing cells. On the other hand, no significant difference in the cellular distribution of the inactive unlipidated compound **21** (0.1 μM) in the two cell lines was observed (Figure 7A and B). This suggests that compound **20** interacts directly with FPR2, and that this is causing the difference in localization between compound **20** and its non-lipidated analogue. This conclusion is supported by the fact that compound **21** binds equally well to the two transfectants, whereas compound **20** displays a 2-fold higher binding to the FPR2 transfectants. These results indicate that FPR2-inhibiting lipidated peptidomimetics interacts with the receptor, and to investigate whether this interaction affects agonist binding, we performed a classical binding competition experiment in which the binding of a fluorescently labeled FPR1 agonist (FITC-fNLFNYK) and an FPR2 agonist (Cy5-WKYMWM) were evaluated. Compound **1** (0.01 – 0.2 μM) dose-dependently inhibited binding of the FPR2 ligand, whereas no effect was seen on binding of the FPR1 agonist (Figure 8A and B). No inhibitory effect on neither the FPR1 nor the FPR2 ligand was

found when a non-lipidated inactive analogue (compound **2**) was used as competing agonist (data not shown).

## *4. Discussion*

Host defense peptides and certain peptidomimetics are considered to be promising anti-infective drug leads due to their potent immunomodulatory activity. Here, we report that a proteolytically stable palmitoylated α-peptide/β-peptoid host defense peptide mimic, Pam-(Lys-βNSpe)$_6$-$NH_2$ (compound **1**, Figure 1B), reduces the pro-inflammatory activity of human neutrophils by selective inhibition of signaling through the pattern recognition receptor FPR2. Combining functional data in primary neutrophils, showing that the inhibitory activity of Pam-(Lys-βNSpe)$_6$-$NH_2$ occurs early in the signaling cascade, with imaging techniques and flow cytometry data showing that Pam-(Lys-βNSpe)$_6$-$NH_2$ preferentially interacts with cells expressing FPR2 and blocks the binding of FPR2 ligands, we show that Pam-(Lys-βNSpe)$_6$-$NH_2$ exerts its inhibitory activity through direct interaction with FPR2 or associated molecules. Pam-(Lys-βNSpe)$_6$-$NH_2$ potently inhibits release of oxygen radicals induced by all tested FPR2 ligands comprising pathogen-derived peptides as well as a synthetic pepducin derived from the third intracellular loop of FPR2, i.e. F2Pal10. According to the prevailing hypothesis, pepducins like F2Pal10 [63] become anchored to the cell membrane through insertion of the fatty acid moiety into the lipid bilayer. This triggers the peptide part of the pepducin molecule to "flip" onto the intracellular side of the membrane where they are assumed to exert their agonistic or antagonistic action by allosteric modulation at intracellular domains of the receptor or on associated signaling molecules [61, 62, 65]. Due to this alternative mode of action of pepducins as compared to that of classical agonists, regular

receptor antagonists are not expected to affect activation by pepducins [66]. Therefore, inhibition of F2Pal10-induced stimulation by Pam-(Lys-βNSpe)$_6$-NH$_2$ suggests that it may similarly be an allosteric modulator thereby inhibiting activation by the pepducin agonist F2Pal10. It is worth noticing, however, that PBP10, the FPR2 antagonist WRW$_4$, as well as the S. aureus derived FPR2 antagonist FLIPr also inhibit stimulation by F2Pal10 [63], and thus it remains a possibility that F2Pal10 has another mechanism of action than that elucidated for other pepducins. The FPR2-selective activity of Pam-(Lys-βNSpe)$_6$-NH$_2$ was found to be dependent on the length and position of the conjugated fatty acid as well as the length and the alternating cationic/hydrophobic design of the α-peptide/β-peptoid oligomer backbone. The importance of the fatty acid conjugation for FPR2 inhibition supports the hypothesis that Pam-(Lys- βNSpe)$_6$-NH$_2$ is an allosteric modulator, and suggests that it acts via lipid anchoring to the cell membrane similarly to the pepducins. However, it could also be hypothesized that the lipid moieties of Pam-(Lys-βNSpe)$_6$-NH$_2$ and F2Pal10 are merely facilitating the specific interaction with FPR2 and thus constitute a molecular pattern recognized by FPR2. The potency of Pam-(Lys-βNSpe)$_6$-NH$_2$ as inhibitor of the release of oxygen radicals induced by the FPR2 agonist WKYMWM is similar to the most potent of the previously described FPR2 inhibitors, namely PBP10. These two inhibitors were found to be significantly more potent and to possess a significantly different dose-response profile as compared to the conventional FPR2 antagonist WRW$_4$, indicating that they may work through different mechanisms. Furthermore, combining PBP10 and Pam-(Lys-βNSpe)$_6$-NH$_2$ resulted in an additive effect, and the activity of both compounds was found to be reversible. Also in functional assays such as measurement of neutrophil degranulation and rise in cytosolic free calcium, their effects are similar. Thus, no functional differences between PBP10 and Pam-(Lys- βNSpe)$_6$-NH$_2$ could be established in the present study, and the question of whether

these two inhibitors use similar mechanisms of action remains unresolved. PBP10 is cell-penetrating - a property that has been associated with the conjugated rhodamine moiety which is essential for its FPR2-inhibitory activity [53]. Likewise, peptidomimetics with α-peptide/β-peptoid backbones, like Pam-(Lys-βNSpe)$_6$-NH$_2$, have previously been shown to be internalized into mammalian HeLa cells [67, 68]. In the present study this ability was extended to comprise immune cells as well, since imaging flow cytometry data showed that a fluorescently labeled non-lipidated analogue (compound **21,** figure 1B) was readily internalized into human neutrophils and HL60 cells. However, compound **21** was found to be inactive in functional assays for FPR2 inhibition, indicating that efficient cellular internalization is not linked to FPR2 inhibition. In agreement with this observation the palmitoyl moiety of Pam-(Lys- βNSpe)$_6$-NH$_2$ was found to be crucial for FPR2 inhibition, and it was required for an efficient interaction between Pam-(Lys-βNSpe)$_6$-NH$_2$ (or the fluorophore-labeled analogue compound **20**) and FPR2. Previously it has been shown that the rhodamine group in PBP10 cannot be exchanged for palmitic acid [53], indicating that Pam-(Lys-βNSpe)$_6$-NH$_2$ and PBP10 might not use identical mechanisms of action. Furthermore, although cellular internalization has been shown for both inhibitors, it is not known whether they exert their action intra- or extracellularly. The rapid reversibility of their inhibitory effects (complete reversal within 1 min) after dilution to ineffective concentrations of the compounds indicates an extracellular mode of action, since the halftimes for cellular uptake of classical cell-penetrating peptides are typically in the range of minutes to hours [69].Several natural as well as synthetic HDPs have been shown to, directly or indirectly, activate human neutrophils, an effect that has been hypothesized to be important for their in vivo antimicrobial activity and beneficial effect in experimental sepsis [37-39, 70]. This stimulatory effect, has for some HDPs, e.g. LL-37 and IDR-1002, been linked to activation of

FPR2 [39, 40, 70]. On the other hand, increased ROS production by neutrophils has been associated with poor outcomes in sepsis patients [71] and mouse studies have implicated endogenous FPR2 agonists in sepsis development [72]. Pam-(Lys-βNSpe)$_6$-$NH_2$ is, to our knowledge, the first HDP mimic that has been shown to inhibit stimulation through FPR2. This makes Pam-(Lys-βNSpe)$_6$-$NH_2$ a convenient tool for the further dissection of the role of FPR2 during infection and inflammation, and the role of neutrophil stimulation in anti-sepsis therapy with HDPs. Furthermore, we consider Pam-(Lys-βNSpe)$_6$-$NH_2$ to be a promising lead compound for development of novel anti-inflammatory drugs.

**Acknowledgements**

We thank the members of the Phagocyte Research Group at the Sahlgrenska Academy for critically discussing the results and the manuscript. Sarah Line Skovbakke is supported by generous research grants from Department of Drug Design and Pharmacology, University of Copenhagen, Aase and Ejnar Danielsens foundation and King Christian 10$^{th}$ foundation. The ImageStreamX was purchased after funding from IngaBritt and Arne Lundbergs foundation. The funding agencies had no influence on the study design, data collection and analysis, or writing and submission of the report.

## *References*

[1] Tosi MF. Innate immune responses to infection. J Allergy Clin Immunol. 2005;116:241-9.

[2] Suresh R, Mosser DM. Pattern recognition receptors in innate immunity, host defense, and immunopathology. Adv Physiol Educ. 2013;37:284-91.

[3] Remick DG. Pathophysiology of sepsis. Am J Pathol. 2007;170:1435-44.

[4] Stearns-Kurosawa DJ, Osuchowski MF, Valentine C, Kurosawa S, Remick DG. The pathogenesis of sepsis. Annu Rev Pathol. 2011;6:19-48.

[5] Castellheim A, Brekke OL, Espevik T, Harboe M, Mollnes TE. Innate immune responses to danger signals in systemic inflammatory response syndrome and sepsis. Scand J Immunol. 2009;69:479-91.

[6] Braine T. Race against time to develop new antibiotics. Bull WHO. 2011;89:88-9.

[7] Fischbach MA, Walsh CT. Antibiotics for emerging pathogens. Science. 2009;325:1089-93.

[8] Livermore DM. Has the era of untreatable infections arrived? J Antimicrob Chemother. 2009;64 Suppl 1:i29-36.

[9] Finlay BB, Hancock RE. Can innate immunity be enhanced to treat microbial infections? Nature Rev Microbiol. 2004;2:497-504.

[10] Hancock RE, Nijnik A, Philpott DJ. Modulating immunity as a therapy for bacterial infections. Nature Rev Microbiol. 2012;10:243-54.

[11] Nijnik A, Hancock R. Host defence peptides: antimicrobial and immunomodulatory activity and potential applications for tackling antibiotic-resistant infections. Emerg Health Threat J. 2009;2:e1.

[12] Yount NY, Bayer AS, Xiong YQ, Yeaman MR. Advances in antimicrobial peptide immunobiology. Biopolym. 2006;84:435-58.

[13] Kovach MA, Standiford TJ. The function of neutrophils in sepsis. Curr Opin Infect Dis. 2012;25:321-7.

[14] Ma AC, Kubes P. Platelets, neutrophils, and neutrophil extracellular traps (NETs) in sepsis. J Thromb Haemost. 2008;6:415-20.

[15] Drifte G, Dunn-Siegrist I, Tissieres P, Pugin J. Innate Immune Functions of Immature Neutrophils in Patients With Sepsis and Severe Systemic Inflammatory Response Syndrome. Crit Care Med. 2013;41:820-32.

[16] Yu Y, Su K. Neutrophil Extracellular Traps and Systemic Lupus Erythematosus. J Clin Cell Immunol. 2013;4:pii 139.

[17] Kumar V, Sharma A. Neutrophils: Cinderella of innate immune system. Int Immunopharmacol. 2010;10:1325-34.

[18] Mantovani A, Cassatella MA, Costantini C, Jaillon S. Neutrophils in the activation and regulation of innate and adaptive immunity. Nature Rev Immunol. 2011;11:519-31.

[19] Futosi K, Fodor S, Mocsai A. Neutrophil cell surface receptors and their intracellular signal transduction pathways. Int Immunopharmacol. 2013;17:638-50.

[20] Ye RD, Boulay F, Wang JM, Dahlgren C, Gerard C, Parmentier M, et al. International Union of Basic and Clinical Pharmacology. LXXIII. Nomenclature for the formyl peptide receptor (FPR) family. Pharmacol Rev. 2009;61:119-61.

[21] Sogawa Y, Ohyama T, Maeda H, Hirahara K. Inhibition of neutrophil migration in mice by mouse formyl peptide receptors 1 and 2 dual agonist: indication of cross-desensitization in vivo. Immunol. 2011;132:441-50.

[22] Blackwood RA, Hartiala KT, Kwoh EE, Transue AT, Brower RC. Unidirectional heterologous receptor desensitization between both the fMLP and C5a receptor and the IL-8 receptor. J Leukoc Biol. 1996;60:88-93.

[23] Forsman H, Onnheim K, Andreasson E, Christenson K, Karlsson A, Bylund J, et al. Reactivation of desensitized formyl peptide receptors by platelet activating factor: a novel receptor cross talk mechanism regulating neutrophil superoxide anion production. PloS one. 2013;8:e60169.

[24] Onnheim K, Christenson K, Gabl M, Burbiel JC, Muller CE, Oprea TI, et al. A novel receptor cross-talk between the ATP receptor P2Y2 and formyl peptide receptors reactivates desensitized neutrophils to produce superoxide. Exp Cell Res. 2014;323:209-17.

[25] Zhang Q, Raoof M, Chen Y, Sumi Y, Sursal T, Junger W, et al. Circulating mitochondrial DAMPs cause inflammatory responses to injury. Nature. 2010;464:104-7.

[26] Chen K, Liu M, Liu Y, Yoshimura T, Shen W, Le Y, et al. Formylpeptide receptor-2 contributes to colonic epithelial homeostasis, inflammation, and tumorigenesis. J Clin Invest. 2013;123:1694-704.

[27] Dufton N, Hannon R, Brancaleone V, Dalli J, Patel HB, Gray M, et al. Anti-inflammatory role of the murine formyl-peptide receptor 2: ligand-specific effects on leukocyte responses and experimental inflammation. J Immunol. 2010;184:2611-9.

[28] Chen K, Le Y, Liu Y, Gong W, Ying G, Huang J, et al. A critical role for the g protein-coupled receptor mFPR2 in airway inflammation and immune responses. J Immunol. 2010;184:3331-5.

[29] Wenceslau CF, McCarthy CG, Goulopoulou S, Szasz T, NeSmith EG, Webb RC. Mitochondrial-derived N-formyl peptides: novel links between trauma, vascular collapse and sepsis. Med hypotheses. 2013;81:532-5.

[30] Dufton N, Perretti M. Therapeutic anti-inflammatory potential of formyl-peptide receptor agonists. Pharmacol Ther. 2010;127:175-88.

[31] Cevik-Aras H, Kalderen C, Jenmalm Jensen A, Oprea T, Dahlgren C, Forsman H. A non-peptide receptor inhibitor with selectivity for one of the neutrophil formyl peptide receptors, FPR 1. Biochem Pharmacol. 2012;83:1655-62.

[32] Stenfeldt AL, Karlsson J, Wenneras C, Bylund J, Fu H, Dahlgren C. Cyclosporin H, Boc-MLF and Boc-FLFLF are antagonists that preferentially inhibit activity triggered through the formyl peptide receptor. Inflamm. 2007;30:224-9.

[33] Forsman H, Dahlgren C. The FPR2-induced rise in cytosolic calcium in human neutrophils relies on an emptying of intracellular calcium stores and is inhibited by a gelsolin-derived PIP2-binding peptide. BMC Cell Biol. 2010;11:52.

[34] Fu H, Bjorkman L, Janmey P, Karlsson A, Karlsson J, Movitz C, et al. The two neutrophil members of the formylpeptide receptor family activate the NADPH-oxidase through signals that differ in sensitivity to a gelsolin derived phosphoinositide-binding peptide. BMC Cell Biol. 2004;5:50.

[35] Zheng Y, Niyonsaba F, Ushio H, Ikeda S, Nagaoka I, Okumura K, et al. Microbicidal protein psoriasin is a multifunctional modulator of neutrophil activation. Immunol. 2008;124:357-67.

[36] Zheng Y, Niyonsaba F, Ushio H, Nagaoka I, Ikeda S, Okumura K, et al. Cathelicidin LL-37 induces the generation of reactive oxygen species and release of human α-defensins from neutrophils. Brit J Dermatol. 2007;157:1124-31.

[37] Alalwani SM, Sierigk J, Herr C, Pinkenburg O, Gallo R, Vogelmeier C, et al. The antimicrobial peptide LL-37 modulates the inflammatory and host defense response of human neutrophils. Eur J Immunol. 2010;40:1118-26.

[38] Niyonsaba F, Madera L, Afacan N, Okumura K, Ogawa H, Hancock RE. The innate defense regulator peptides IDR-HH2, IDR-1002, and IDR-1018 modulate human neutrophil functions. J Leukoc Biol. 2013; 94:159-70.

[39] De Y, Chen Q, Schmidt AP, Anderson GM, Wang JM, Wooters J, et al. LL-37, the neutrophil granule- and epithelial cell-derived cathelicidin, utilizes formyl peptide receptor-like 1 (FPRL1) as a receptor to chemoattract human peripheral blood neutrophils, monocytes, and T cells. J Exp Med. 2000;192:1069-74.

[40] Tjabringa GS, Ninaber DK, Drijfhout JW, Rabe KF, Hiemstra PS. Human cathelicidin LL-37 is a chemoattractant for eosinophils and neutrophils that acts via formyl-peptide receptors. Int Arch Allergy Immunol. 2006;140:103-12.

[41] Lee HY, Bae YS. The anti-infective peptide, innate defense-regulator peptide, stimulates neutrophil chemotaxis via a formyl peptide receptor. Biochem Biophys Res Commun. 2008;369:573-8.

[42] Hancock RE, Sahl HG. Antimicrobial and host-defense peptides as new anti-infective therapeutic strategies. Nat Biotechnol. 2006;24:1551-7.

[43] Olsen CA, Bonke G, Vedel L, Adsersen A, Witt M, Franzyk H, et al. α-peptide/β-peptoid chimeras. Org Lett. 2007;9:1549-52.

[44] Thaker HD, Som A, Ayaz F, Lui D, Pan W, Scott RW, et al. Synthetic mimics of antimicrobial peptides with immunomodulatory responses. J Am Chem Soc. 2012;134:11088-91.

[45] Som A, Navasa N, Percher A, Scott RW, Tew GN, Anguita J. Identification of Synthetic Host Defense Peptide Mimics that Exert Dual Antimicrobial and Anti-Inflammatory Activities. Clin Vaccine Immunol. 2012;19:1784-91.

[46] Jahnsen RD, Frimodt-Moller N, Franzyk H. Antimicrobial activity of peptidomimetics against multidrug-resistant Escherichia coli: a comparative study of different backbones. J Med Chem. 2012;55:7253-61.

[47] Jahnsen RD, Haney EF, Franzyk H, Hancock RE. Characterization of a Proteolytically Stable Multifunctional Host Defense Peptidomimetic. Chem Biol. 2013;20:1286-95.

[48] Vedel L, Bonke G, Foged C, Ziegler H, Franzyk H, Jaroszewski JW, et al. Antiplasmodial and prehemolytic activities of α-peptide-β-peptoid chimeras. ChemBioChem. 2007;8:1781-4.

[49] Liu Y, Knapp KM, Yang L, Molin S, Franzyk H, Folkesson A. High in vitro antimicrobial activity of β-peptoid-peptide hybrid oligomers against planktonic and biofilm cultures of *Staphylococcus epidermidis*. Int J Antimicrob Agents. 2013;41:20-7.

[50] Gitte Bonke LV, Matthias Witt, Jerzy W. Jaroszewski, Christian A. Olsen, Henrik Franzyk. Dimeric building blocks for solid-phase synthesis of α-peptide-β-peptoid chimeras. Synthesis. 2008;15:2381-90.

[51] Kruijtzer JAW, Hofmeyer LJF, Heerma W, Versluis C, Liskamp RMJ. Solid-phase syntheses of peptoids using Fmoc-protected N-substituted glycines: The synthesis of (retro) peptoids of Leu-enkephalin and substance P. Chem-Eur J. 1998;4:1570-80.

[52] Christophe T, Karlsson A, Dugave C, Rabiet MJ, Boulay F, Dahlgren C. The synthetic peptide Trp-Lys-Tyr-Met-Val-Met-NH2 specifically activates neutrophils through FPRL1/lipoxin A4 receptors and is an agonist for the orphan monocyte-expressed chemoattractant receptor FPRL2. J Biol Chem. 2001;276:21585-93.

[53] Forsman H, Andreasson E, Karlsson J, Boulay F, Rabiet MJ, Dahlgren C. Structural characterization and inhibitory profile of formyl peptide receptor 2 selective peptides descending from a PIP2-binding domain of gelsolin. J Immunol. 2012;189:629-37.

[54] Lundqvist H, Dahlgren C. Isoluminol-enhanced chemiluminescence: a sensitive method to study the release of superoxide anion from human neutrophils. Free Radic Biol Med. 1996;20:785-92.

[55] Dahlgren C, Karlsson A. Respiratory burst in human neutrophils. J Immunol Methods. 1999;232:3-14.

[56] Bylund J, Bjorstad A, Granfeldt D, Karlsson A, Woschnagg C, Dahlgren C. Reactivation of formyl peptide receptors triggers the neutrophil NADPH-oxidase but not a transient rise in intracellular calcium. J Biol Chem. 2003;278:30578-86.

[57] Huet E, Boulay F, Barral S, Rabiet MJ. The role of beta-arrestins in the formyl peptide receptor-like 1 internalization and signaling. Cell Signal. 2007;19:1939-48.

[58] Hendriks-Balk MC, Peters SL, Michel MC, Alewijnse AE. Regulation of G protein-coupled receptor signalling: focus on the cardiovascular system and regulator of G protein signalling proteins. Eur J Pharmacol. 2008;585:278-91.

[59] Klein C, Paul JI, Sauve K, Schmidt MM, Arcangeli L, Ransom J, et al. Identification of surrogate agonists for the human FPRL-1 receptor by autocrine selection in yeast. Nature Biotechnol. 1998;16:1334-7.

[60] Forsman H, Christenson K, Bylund J, Dahlgren C. Receptor-dependent and -independent immunomodulatory effects of phenol-soluble modulin peptides from Staphylococcus aureus on human neutrophils are abrogated through peptide inactivation by reactive oxygen species. Infect Immun. 2012;80:1987-95.

[61] Covic L, Gresser AL, Talavera J, Swift S, Kuliopulos A. Activation and inhibition of G protein-coupled receptors by cell-penetrating membrane-tethered peptides. Proc Natl Acad Sci USA. 2002;99:643-8.

[62] O'Callaghan K, Kuliopulos A, Covic L. Turning receptors on and off with intracellular pepducins: new insights into G-protein-coupled receptor drug development. J Biol Chem. 2012;287:12787-96.

[63] Forsman H, Bylund J, Oprea TI, Karlsson A, Boulay F, Rabiet MJ, et al. The leukocyte chemotactic receptor FPR2, but not the closely related FPR1, is sensitive to cell-penetrating pepducins with amino acid sequences descending from the third intracellular receptor loop. Biochim biophys acta. 2013;1833:1914-23.

[64] Bae YS, Lee HY, Jo EJ, Kim JI, Kang HK, Ye RD, et al. Identification of peptides that antagonize formyl peptide receptor-like 1-mediated signaling. J Immunol. 2004;173:607-14.

[65] Tsuji M, Ueda S, Hirayama T, Okuda K, Sakaguchi Y, Isono A, et al. FRET-based imaging of transbilayer movement of pepducin in living cells by novel intracellular bioreductively activatable fluorescent probes. Org Biomol Chem. 2013;11:3030-7.

[66] Lee HY, Kim SD, Shim JW, Kim HJ, Kwon JY, Kim JM, et al. Activation of human monocytes by a formyl peptide receptor 2-derived pepducin. FEBS letters. 2010;584:4102-8.

[67] Foged C, Franzyk H, Bahrami S, Frokjaer S, Jaroszewski JW, Nielsen HM, et al. Cellular uptake and membrane-destabilising properties of α-peptide/β-peptoid chimeras: lessons for the design of new cell-penetrating peptides. Biochim Biophys Acta. 2008;1778:2487-95.

[68] Jing X, Yang M, Kasimova MR, Malmsten M, Franzyk H, Jorgensen L, et al. Membrane adsorption and binding, cellular uptake and cytotoxicity of cell-penetrating peptidomimetics with α-peptide/β-peptoid backbone: effects of hydrogen bonding and α-chirality in the β-peptoid residues. Biochim Biophys Acta. 2012;1818:2660-8.

[69] Zorko M, Langel U. Cell-penetrating peptides: mechanism and kinetics of cargo delivery. Adv Drug Deliv Rev. 2005;57:529-45.

[70] Nijnik A, Madera L, Ma S, Waldbrook M, Elliott MR, Easton DM, et al. Synthetic cationic peptide IDR-1002 provides protection against bacterial infections through chemokine induction and enhanced leukocyte recruitment. J Immunol. 2010;184:2539-50.

[71] Santos SS, Brunialti MK, Rigato O, Machado FR, Silva E, Salomao R. Generation of nitric oxide and reactive oxygen species by neutrophils and monocytes from septic patients and association with outcomes. Shock. 2012;38:18-23.

[72] Sordi R, Menezes-de-Lima O, Jr., Horewicz V, Scheschowitsch K, Santos LF, Assreuy J. Dual role of lipoxin A4 in pneumosepsis pathogenesis. Int Immunopharmacol. 2013;17:283-92.

[73] Findlay B, Mookherjee N, Schweizer F. Ultrashort cationic lipopeptides and lipopeptoids selectively induce cytokine production in macrophages. PloS one. 2013;8:e54280.

## *Legends*

**Figure 1:** *The chemical structure of residues and compounds used. (A)* α-peptide, α-peptoid, and β-peptoid amino acids as well as the β-peptoid residues βNSpe and βNphe (used in the compounds displayed in B) are shown. *(B)* Overview of the lipidated α-peptide/β-peptoid chimeric oligomers used in this study. Compound 18 and 19 was designed as in [73].

**Figure 2:** *Compound **1** inhibits WKYMWM mediated release of ROS and degranulation. (A)* PMNs were preincubated (37°C, 5 min.) in the presence (broken line) or absence (solid line) of compound **1** (Cmp. 1, 1.0 μM) and stimulated with the FPR1-selective agonist fMLF (0.1 μM), the FPR2-selective agonist WKYMWM (0.1 μM), or PMA (0,05 μM) and the release of superoxide anion was measured immediately. The graph shows representative data from more than three independent experiments. *(B)* PMNs were incubated (37°C, 20 min.) with WKYMWM (0.1 μM) or fMLF (0.1 μM), in the presence or absence of the FPR2 inhibitors PBP10 (1 μM) and compound **1** (Cmp. 1, 0.5 μM). After incubation the cells were stained for cell surface expression of CD11b and analyzed by flow cytometry. The histograms show representative data, and the bar graph shows mean +SD of the CD11b expression in samples with agonists as percentage of the 37°C control sample from three independent experiments. Asterisks indicate statistically significant differences based on a One-way ANOVA with the sample without inhibitors as control sample and Dunnett's test for multiple comparisons. *: $p \leq 0.05$, **: $p \leq 0.01$, ***.

**Fig. 3:** *The inhibitory effect of compound **1** applies to conventional FPR2 agonists and an FPR2-derived pepducin. (A)* PMNs were preincubated (37°C, 5 min.) in the presence or absence of compound **1** (Cmp. **1**, 0.5 μM) and/or cyclosporine H (CsH, 1 μM)) and stimulated with the FPR1 agonists fMLF (0.1 μM) or compound 43 (Cmp. 43, 1 μM), the dual FPR1 and FPR2 agonist WKYMWm (0.05 μM), or the FPR2 agonists WKYMWM (0.1 μM), MMK 1 (0.2 μM), or PSMα2 (0.1 μM) and the release of superoxide anion was measured immediately. The bar graph shows the mean + SD of oxygen release in samples containing inhibitors (Cmp. **1** and CsH) as percentage of samples without inhibitors from four independent experiments. The absolute values of ROS release induced by the various ligands were donor dependent but ranged between: WKYMWM (30-90 mcpm), fMLF (35-90 mcpm), MMK1 (20-70 mcpm), Cmp. 43 (40-80 mcpm), WKYMWm (50-125 mcpm), PSMα2 (6-125 mcpm). Asterisks indicate statistically significant differences based on a One-way ANOVA with the samples stimulated with fMLF or Cmp. 43 as control samples and Dunnett's test for multiple comparisons. *: $p \leq 0.05$, **: $p \leq 0.01$, ***$\leq 0.001$. *(B)* PMNs were preincubated (37°C, 5 min.) in the presence or absence of compound **1** (Cmp. 1, 0.5 μM) and stimulated with the FPR2 derived pepducin F2Pal10 (0.5 μM) and the release of superoxide anion was measured immediately. The kinetic graph shows representative data, whereas the bar graph shows mean + SD of the maximum release of oxygen radicals from four independent experiments. Asterisks indicate statistically significant differences based on a paired t-test. **: $p \leq 0.01$.

**Figure 4:** *Compound **1** inhibits FPR2-mediated mobilization of intracellular calcium. (A)* Fura 2-AM–labeled PMNs were preincubated (10 min at 37°C) with (broken line) or without (solid line) compound **1** (Cmp. 1, 1 μM), after which the cells were stimulated with WKYMWM (black) or fMLF (light gray) (0.02 μM; added at arrow) and the change in intracellular calcium was determined. The graph shows representative data from three independent experiments. The maximum change in intracellular calcium (ΔFura2 fluorescence ratio) was determined by addition of Triton X100 and was found to be 4.5. *(B)* Fura 2-AM–labeled PMNs were preincubated (10 min at 37°C) with or without compound **1** (Cmp. **1**) in varying concentration, after which the cells were stimulated with WKYMWM (white) (0.02 μM) and the change in intracellular calcium was determined. The bar graph shows the mean +SD of the magnitude of the change in $[Ca^{2+}]_i$ from three independent experiments. Asterisks indicate statistically significant differences evaluated by one-way ANOVA with Tukeys multiple comparison test. **: $p \leq 0.01$. The maximum change in intracellular calcium (ΔFura2 fluorescence ratio) was determined by addition of Triton X100 and was found to be 4.5. *(C)* Fura 2-AM labeled HL60 cells stably transfected with either FPR1 or FPR2 were preincubated (10 min at 37°C) in the presence or absence of the FPR1 specific inhibitor CsH (1 μM), the FPR2 specific inhibitor PBP10 (1 μM), or compound **1** (Cmp. 1, 1 μM), after which they were stimulated with 0.02 μM fMLF (FPR1-transfected cells) or WKYMWM (FPR2-transfected cells), and the change in intracellular calcium concentration was determined. The bar graphs show mean +SD of the magnitude of the change in intracellular calcium concentration in the presence of inhibitors as percentage of the samples with no inhibitors from three independent experiments. The absolute values of the change in intracellular calcium concentration induced by stimulation with FPR agonists varied between experiments but ranged between: fMLF in FPR1 transfected cells (2.25-3.0

ΔFura2 fluorescence ratio), WKYMWM in FPR2 transfected cells (2.0-2.6 ΔFura2 fluorescence ratio). Asterisks indicate statistically significant differences evaluated by one-way ANOVA with Tukeys multiple comparison test. **: $p \leq 0.01$, ***: $p \leq 0.001$.

**Figure 5:** *The potencies and effects of compound **1** and PBP10 are similar. (A)* PMNs were preincubated (37°C, 5 min) in the presence or absence of varying concentrations of compound 1 (Cmp. **1**), PBP10, or $WRW_4$ and stimulated with the FPR2-specific agonist WKYMWM (0.1 μM) before measurement of the release of superoxide anion. The graph shows mean +/- SD of the release of superoxide anion in samples with inhibitor as percentage of samples without from four independent experiments, as a function of the concentration of the inhibitor as well as the regression curves used to determine $IC_{50}$ values. The absolute values of ROS release induced by WKYMWM stimulation of the neutrophils varied between donors, but were in the range of 25-90 mcpm. Asterisks indicate statistically significant differences between Cmp. **1** and $WRW_4$ based on multiple t-tests using the Holm-Sidak method for multiple comparisons *: $p \leq 0.05$. No statistically significant differences were found between PBP10 and Cmp. **1**. The degrees of freedom were 40 for each inhibitor. *(B)* PMNs were preincubated (37°C, 5 min) in the presence or absence of compound 1 (Cmp. **1**) and/or PBP10 before stimulation with WKYMWM (0.1 μM) and measurement of the release of superoxide anion. The graph shows representative data from six independent experiments. (C) PMNs ($1 \times 10^7$cells/mL) were preincubated (2 min at room temperature) with or without compound **1** (Cmp. **1**; 0.2 μM) or PBP10 (0.2 μM), The cell suspensions were diluted 100-fold, giving a non-inhibitory concentration of the inhibitors, and after various time periods of recovery the cells were subjected to stimulation with the FPR2-selective peptide WKYMVM (0.1 μM) in the presence (dashed line) or absence (dotted line) of fresh inhibitor (0.2 μM).

**Figure 6:** *A fluorescently-labelled lipidated α-peptide/β-peptoid chimeric oligomer locates to the cell surface of neutrophils. (A)* PMNs were preincubated (37 °C, 5 min) in the presence (broken line) or absence (solid line) of carboxyfluorescein (CF)-labeled lipidated (Cmp. **20**, 0.05 μM) and unlipidated (Cmp. **21**, 0.05 μM) α-peptide/β-peptoid oligomers and stimulated with the FPR1-specific agonist fMLF (0.1 μM) or the FPR2-specific agonist WKYMWM (0.1 μM), and then the release of superoxide anion was measured immediately. *(B-D)* Freshly purified PMNs were stained with compound **20** or **21** (green), before staining of the nucleus with DRAQ5 (red) and analysis by imaging flow cytometry. The data shown are representative for four independent experiments. *(B)* Representative pictures selected around the mean Bright detail intensity (subfigure D) are shown. *(C)* The histogram shows intensity of control PMNs (unlabeled) and PMNs incubated with Cmp. **20** or Cmp. **21**. *(D)* The histogram shows Bright Detail Intensity of PMNs stained with Cmp. **20** or Cmp. **21**.

**Figure 7:** *Selective interaction of a fluorescently-labelled lipidated α-peptide/β-peptoid oligomer with FPR2 in transfected HL60 cells.* HL60 cells stably transfected with either FPR1 or FPR2 were incubated with the carboxyfluorescein (CF)-labelled FPR2 inhibitor Cmp. **20** (green), an inactive unlipidated CF-labelled compound **21** (green), or left untreated, before staining of the nucleus with DRAQ5 (red) and analysis by imaging flow cytometry. Separate cell samples were immunofluorescently stained for the presence of FPR2 (red). The raw data shown in pictures and histograms are representative for three independent experiments. *(A)* Representative pictures selected around the mean Bright detail intensity from one experiment are shown. *(B)* The diagram shows Bright Detail Intensity in the CF-channel +SD from three independent experiments. The histograms show representative data from one experiment. The asterisks indicate statistically significant differences evaluated by two-way ANOVA with

Sidaks method for multiple comparisons. ***: $p \leq 0.001$. *(C)* The diagram shows Mean Fluorescence Intensity (MFI) of cells stained with CF-labeled compounds +SD from three independent experiments. The asterisks indicate statistically significant differences evaluated by two-way ANOVA with Sidaks method for multiple comparisons. **: $p \leq 0.01$. The histograms show representative data from one experiment. The x-axis in histograms is a log-scale.

**Figure 8:** *Compound **1** competes for the binding of FPR2 ligands.* PMNs were preincubated with varying concentrations of compound **1** (Cmp. 1, ice, 5 min) before incubation (ice, 30 min) with Cy5-WKYMWM or FITC-fNLFNYK and analysis by flow cytometry. *(A)* The histograms show representative data for undtained PMNs preincubated with buffer, Cmp. **1** (0.2 μM), or unlabeled ligand (0.5 μM). *(B)* The bar graphs show mean +SD of staining with fluorescently labeled FPR agonists after subtraction of the background fluorescence of unstained cells in the presence of Cmp. **1** as percentage of samples without Cmp. **1** from at least three independent experiments. Asterisks indicate statistically significant differences based on a One-way ANOVA using Tukey's method for multiple comparison. *: $p \leq 0.05$, **: $p \leq 0.01$, *** $p \leq 0.001$.

*Graphical Abstract (for review)

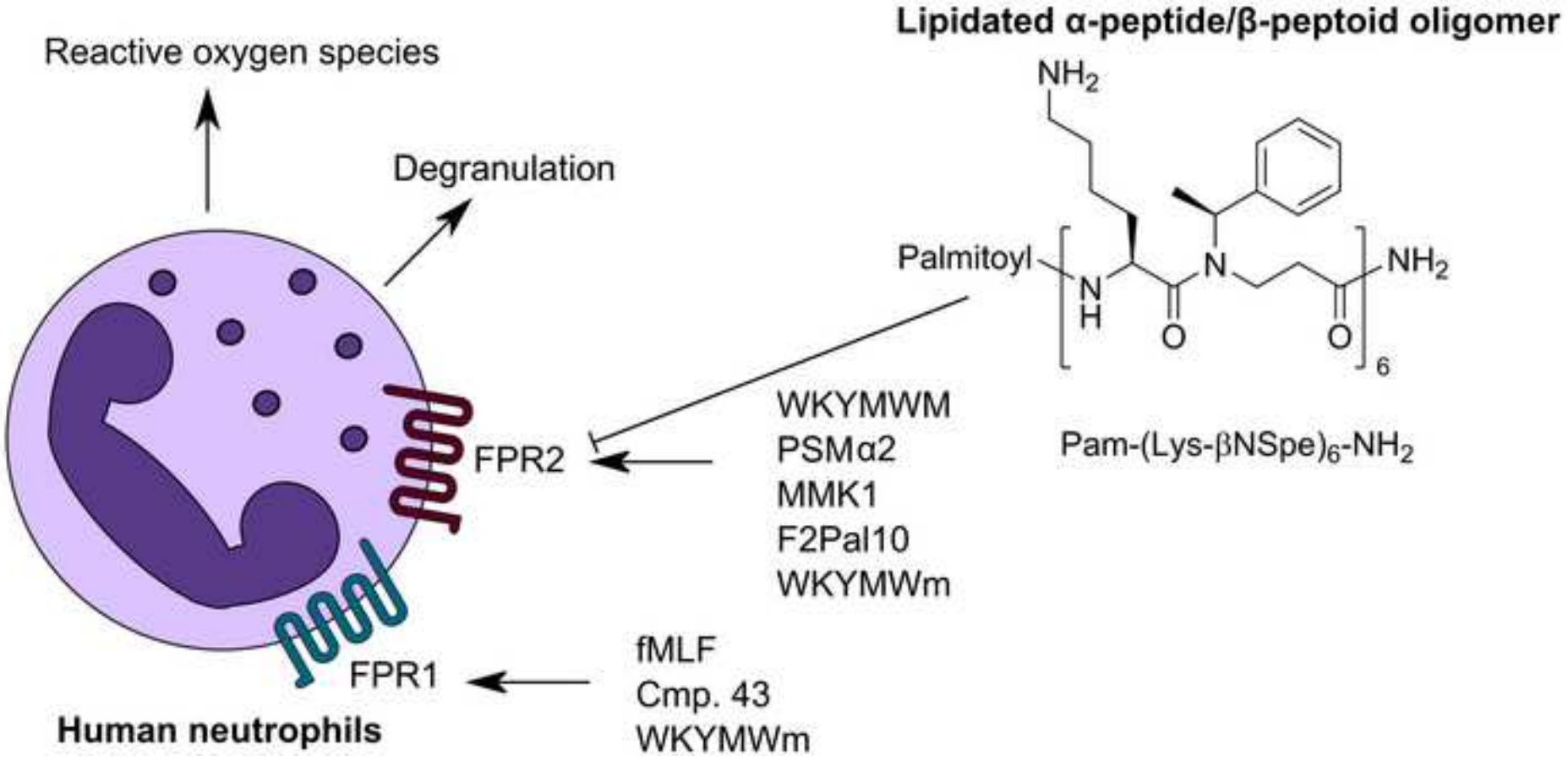

## *Tables*

**Table I:** FPR2 and FPR1 inhibition of structural analogues of compound

| No[1] | Structure | Inhibition of WKYMWM induced ROS secretion $IC_{50}$-value [μM][2] | % inhibition of fMLF[3] induced ROS secretion |
|---|---|---|---|
| **1** | Pam-(Lys-βNSpe)$_6$-$NH_2$ | 0.05 (0.04-0.07) | - |
| | **Effect of lipid length and position** | | |
| **2** | Ac-(Lys-βNSpe)$_6$-$NH_2$ | -[4] | - |
| **3** | Ste-(Lys-βNSpe)$_6$-$NH_2$ | 0.03 (0.02-0.06) | - |
| **4** | Lau-(Lys-βNSpe)$_6$-$NH_2$ | 0.18 (0.14-0.24) | - |
| **5** | Oct-(Lys-βNSpe)$_6$-$NH_2$ | 0.96 (0.6-1.5) | - |
| **6** | Oct-(Lys(Lau))-(Lys-βNSpe)$_6$-$NH_2$ | 0.10 (0.07-0.14) | - |
| **7** | Ac-2-Aoc-(Lys-βNSpe)$_6$-$NH_2$ | >1,0[5] | - |
| **8** | Ac-2-Aoc-2-Aoc-(Lys-βNSpe)$_6$-$NH_2$ | 0.72 (0.49-1.05) | - |
| | **Effect of backbone sequence** | | |
| **9** | Pam-(Lys-βNPhe)$_6$-$NH_2$ | 0.06 (0.04-0.1) | - |
| **10** | Pam-(hArg-βNSpe)$_6$-$NH_2$ | 0.04 (0.02-0.08) | 72 % |
| | **Effect of backbone length** | | |
| **11** | Pam-(Lys-βNSpe-hArg-βNSpe)-$NH_2$ | 0.35 (0.21-0.59) | - |
| **12** | Pam-(Lys-βNSpe-hArg-βNSpe)$_2$-$NH_2$ | 0.05 (0.03-0.07) | 17 % |
| **13** | Pam-(Lys-βNSpe-hArg-βNSpe)$_3$-$NH_2$ | 0.03 (0.02-0.04) | 51 % |
| **14** | Pam-(Lys-βNSpe-hArg-βNSpe)$_4$-$NH_2$ | 0.04 (0.02-0.08) | - |
| **15** | Ac-(Lys-βNSpe-hArg-βNSpe)$_4$-$NH_2$ | 0.47 (0.36-0.61) | - |
| **16** | Ac-(Lys-βNSpe-hArg-βNSpe)-$NH_2$ | -[e] | - |
| | **Lipidated cationic compounds** | | |
| **17** | Pam-(Lys)$_6$ | -[e] | - |
| **18** | Pam-(Lys)$_3$ | -[e] | - |
| **19** | Pam-(NLys)$_3$ | -[e] | - |

[1] As indicated in figure 1

[2] $IC_{50}$ values are calculated based on data from four independent experiments. Brackets show the 95 % confidence interval.

[3] The % inhibition of fMLF induced response upon 5 min pretreatment with 1 μM compound, shown as the mean value from two independent experiments. – indicates no observed inhibition.

[4] The regression did not converge.

[5] Inhibitory effect was found, but the $IC_{50}$ value was out of the tested range.

**A.**

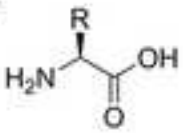

α-amino acid

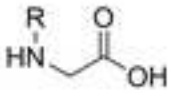

α-peptoid unit

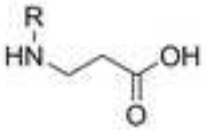

β-peptoid unit

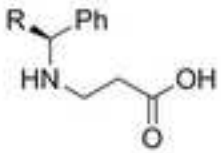

βNspe: R = Me

βNphe: R = H

**B.**

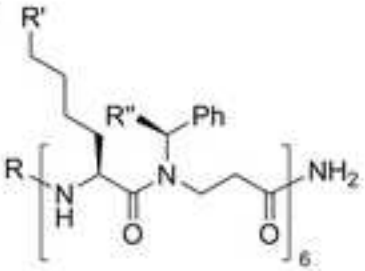

**1** : R = Pam; R' = $NH_2$; R'' = Me

**2** : R = Ac; R' = $NH_2$; R'' = Me

**3** : R = Ste; R' = $NH_2$; R'' = Me

**4** : R = Lau; R' = $NH_2$; R'' = Me

**5** : R = Oct; R' = $NH_2$; R'' = Me

**6** : R = Oct-Lys(Lau); R' = $NH_2$; R'' = Me

**9** : R = Pam; R' = $NH_2$; R'' = H

**10** : R = Pam; R' = NH(C=NH)$NH_2$; R'' = Me

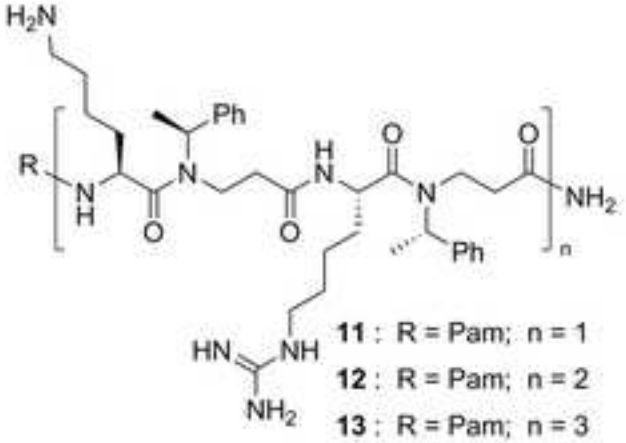

**11** : R = Pam; n = 1

**12** : R = Pam; n = 2

**13** : R = Pam; n = 3

**14** : R = Pam; n = 4

**15** : R = Ac; n = 4

**16** : R = Ac; n = 1

**20** : R = CF-Lys(Pam); n = 3

**21** : R = CF; n = 3

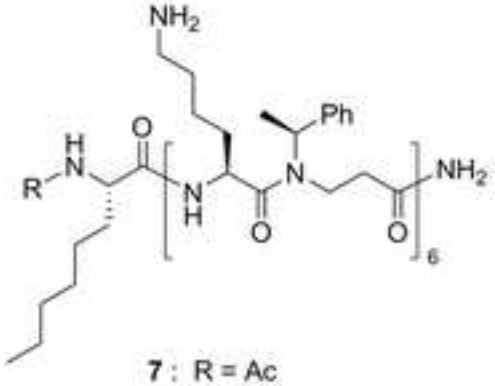

**7** : R = Ac

**8** : R = Ac-(2-Aoc)

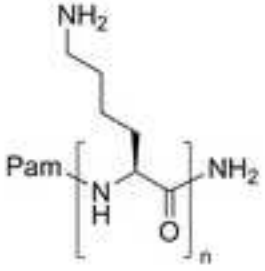

**17** : n = 6

**18** : n = 3

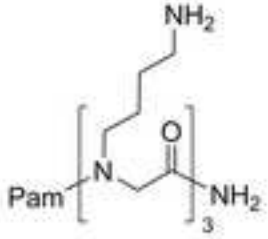

**19**

**Abbreviations used:**

Ac = acetyl

βNSpe: *N*-(S)-phenylethyl-β-alanine

βNphe: *N*-phenyl-β-alanine

CF = 5(6)-carboxyfluoresceinyl

Me = methyl

Ph = phenyl

Oct = octanoyl

Lau = lauryl

Lys(Lau) = *N*-ε-lauryl-Lysine

Lys(Pam) = *N*-ε-palmitoyl-Lysine

Pam = palmitoyl

Ste = steroyl

**Figure 2**

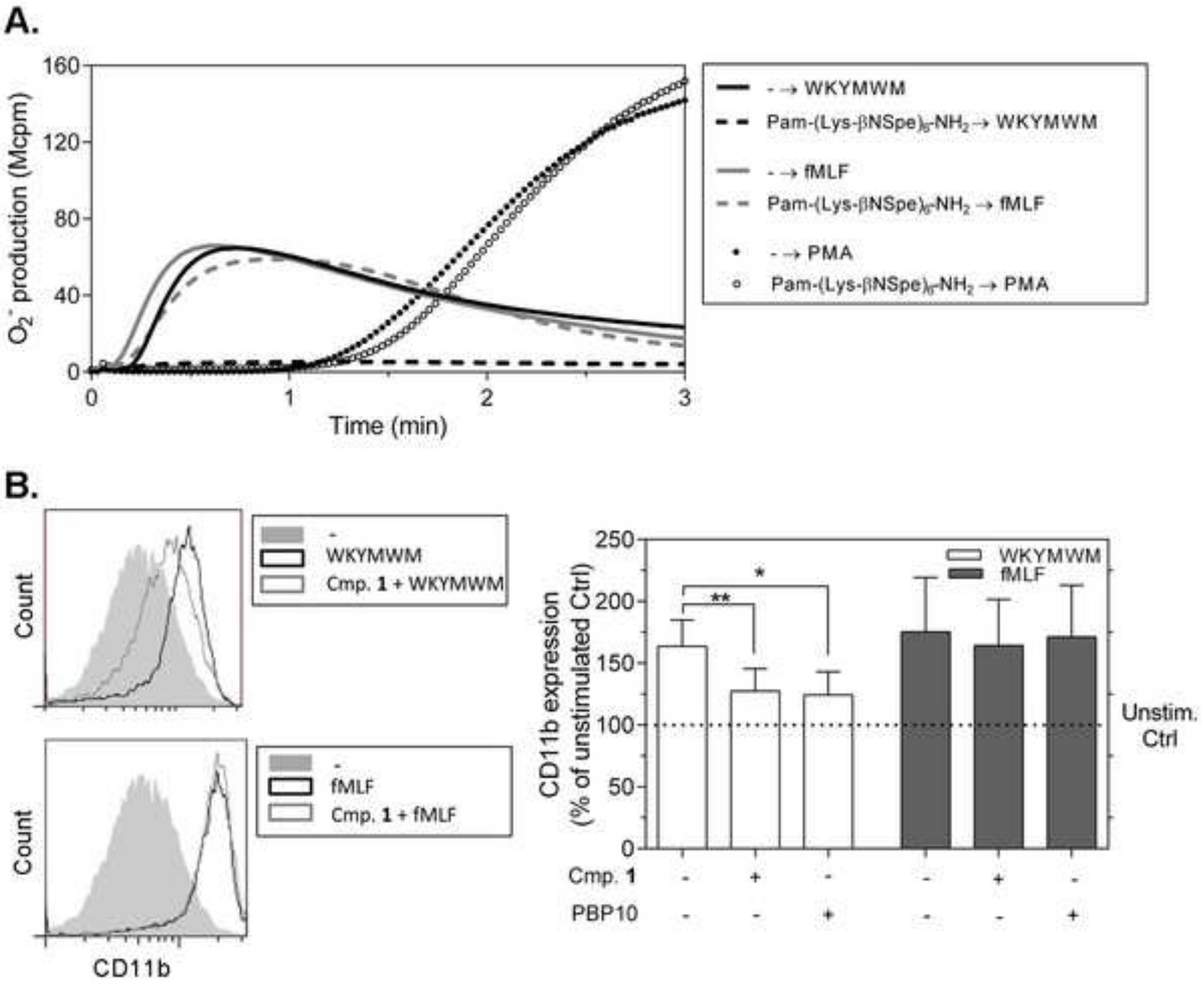
A.
160
120
80
40
0
$O_2^-$ production (Mcpm)
0
1
2
3
Time (min)
- → WKYMWM
Pam-(Lys-βNSpe)$_6$-NH$_2$ → WKYMWM
- → fMLF
Pam-(Lys-βNSpe)$_6$-NH$_2$ → fMLF
- → PMA
Pam-(Lys-βNSpe)$_6$-NH$_2$ → PMA
B.
Count
-
WKYMWM
Cmp. 1 + WKYMWM
Count
-
fMLF
Cmp. 1 + fMLF
CD11b
CD11b expression (% of unstimulated Ctrl)
250
200
150
100
50
0
**
*
WKYMWM
fMLF
Unstim. Ctrl
Cmp. 1
PBP10

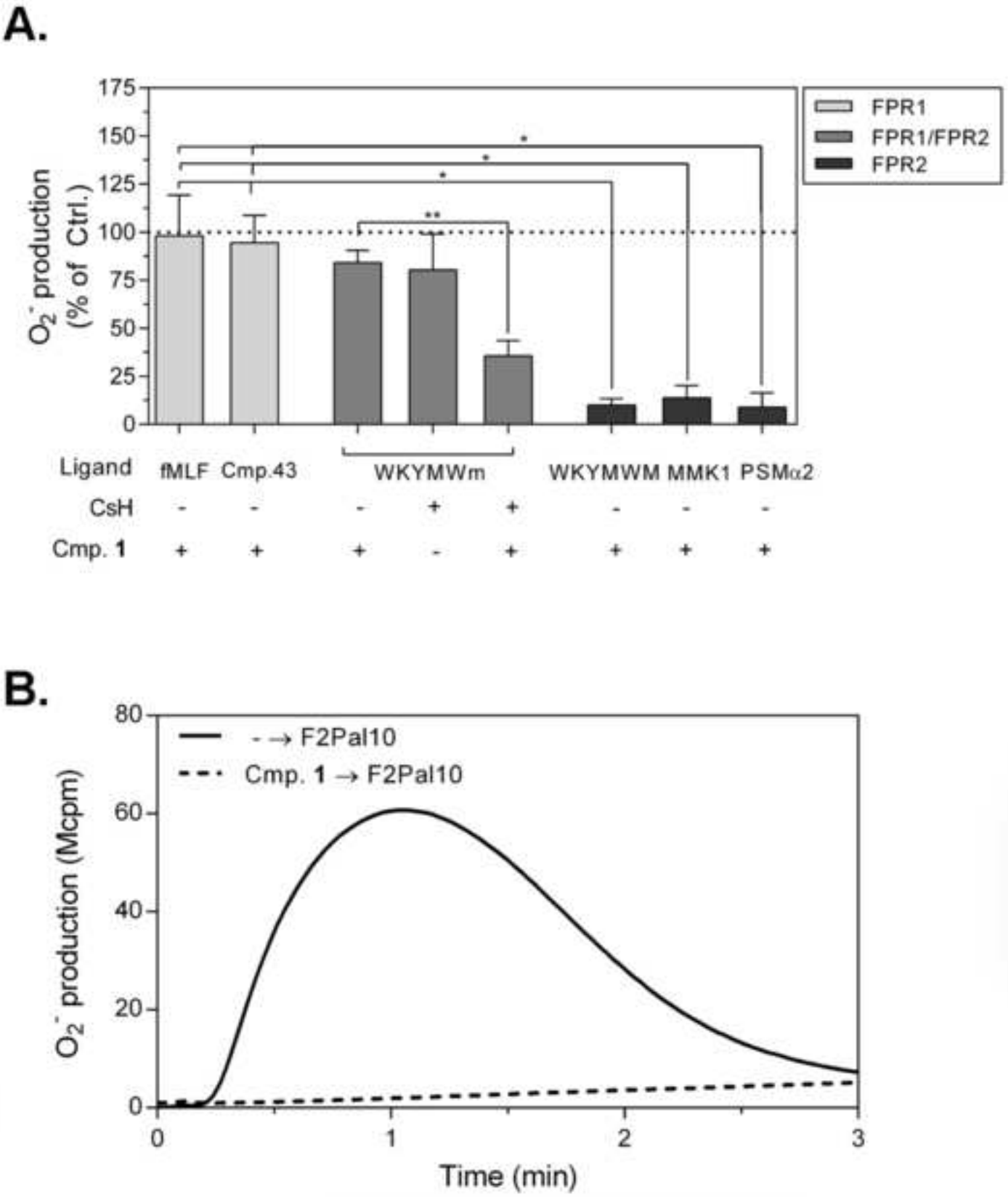

**Figure 4**

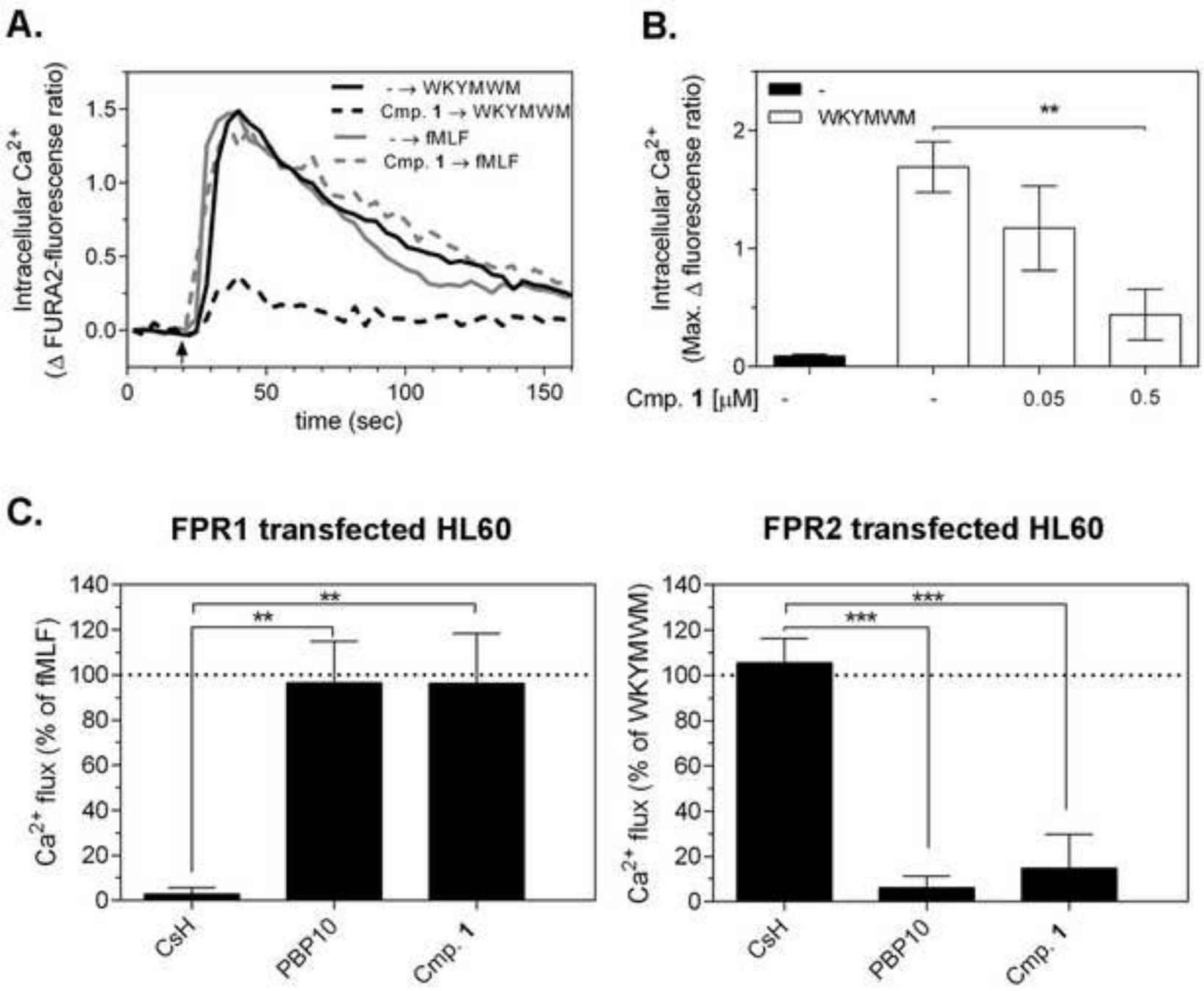
A.
Intracellular Ca2+
(Δ FURA2-fluorescense ratio)
- → WKYMWM
Cmp. 1 → WKYMWM
- → fMLF
Cmp. 1 → fMLF
time (sec)
B.
Intracellular Ca2+
(Max. Δ fluorescense ratio)
WKYMWM
**
Cmp. 1 [μM]
C.
FPR1 transfected HL60
FPR2 transfected HL60
Ca2+ flux (% of fMLF)
Ca2+ flux (% of WKYMWM)
CsH
PBP10
Cmp. 1

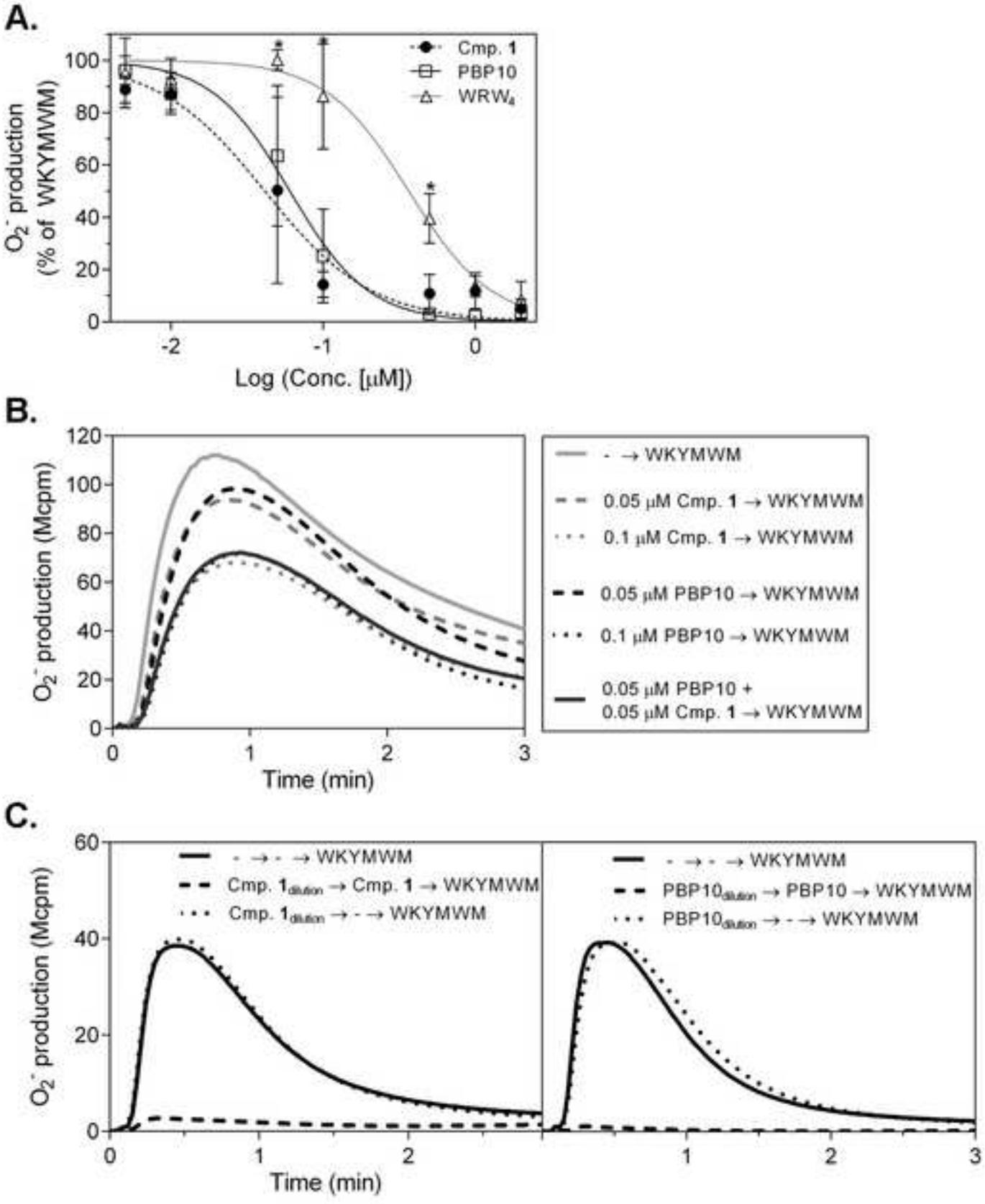

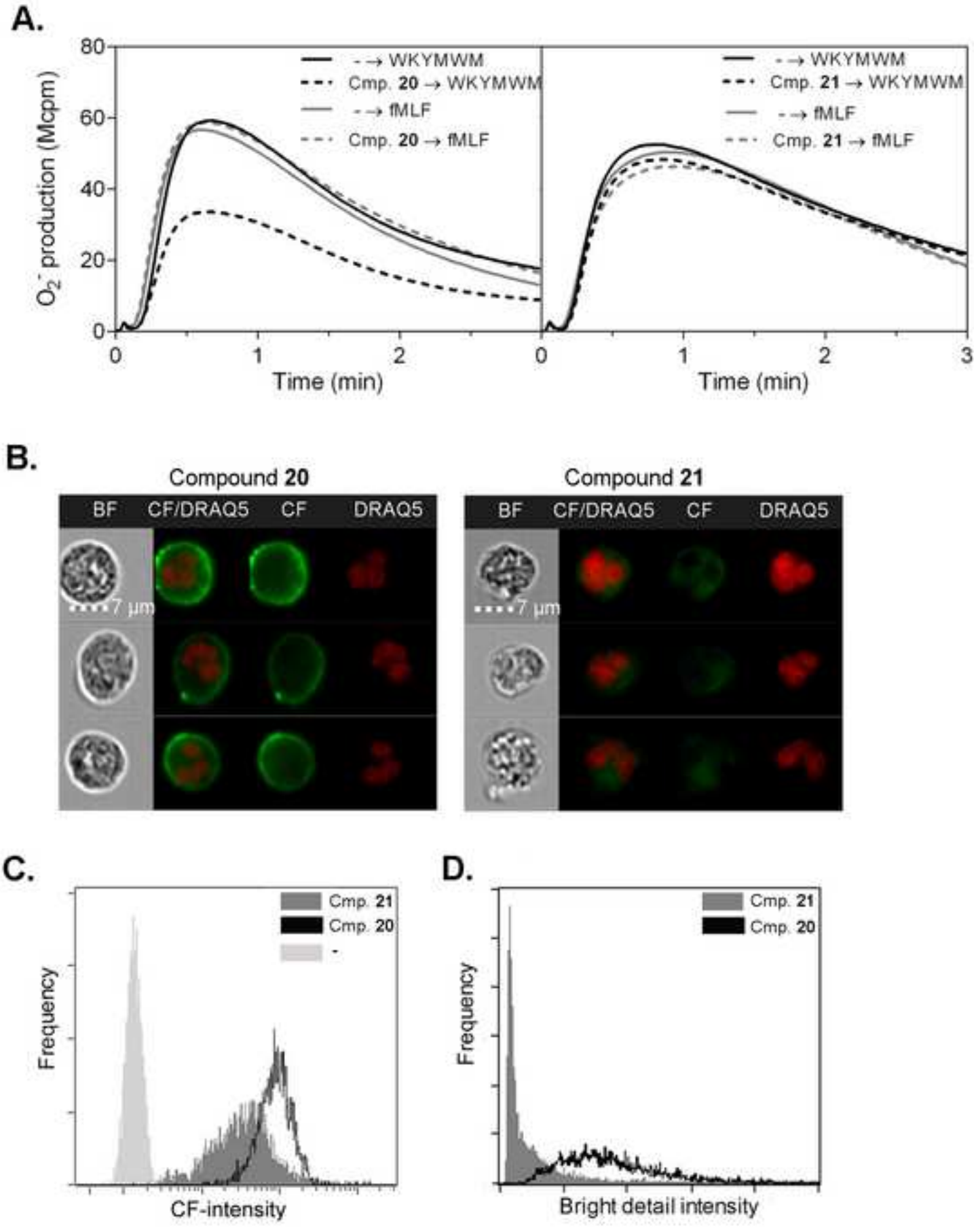

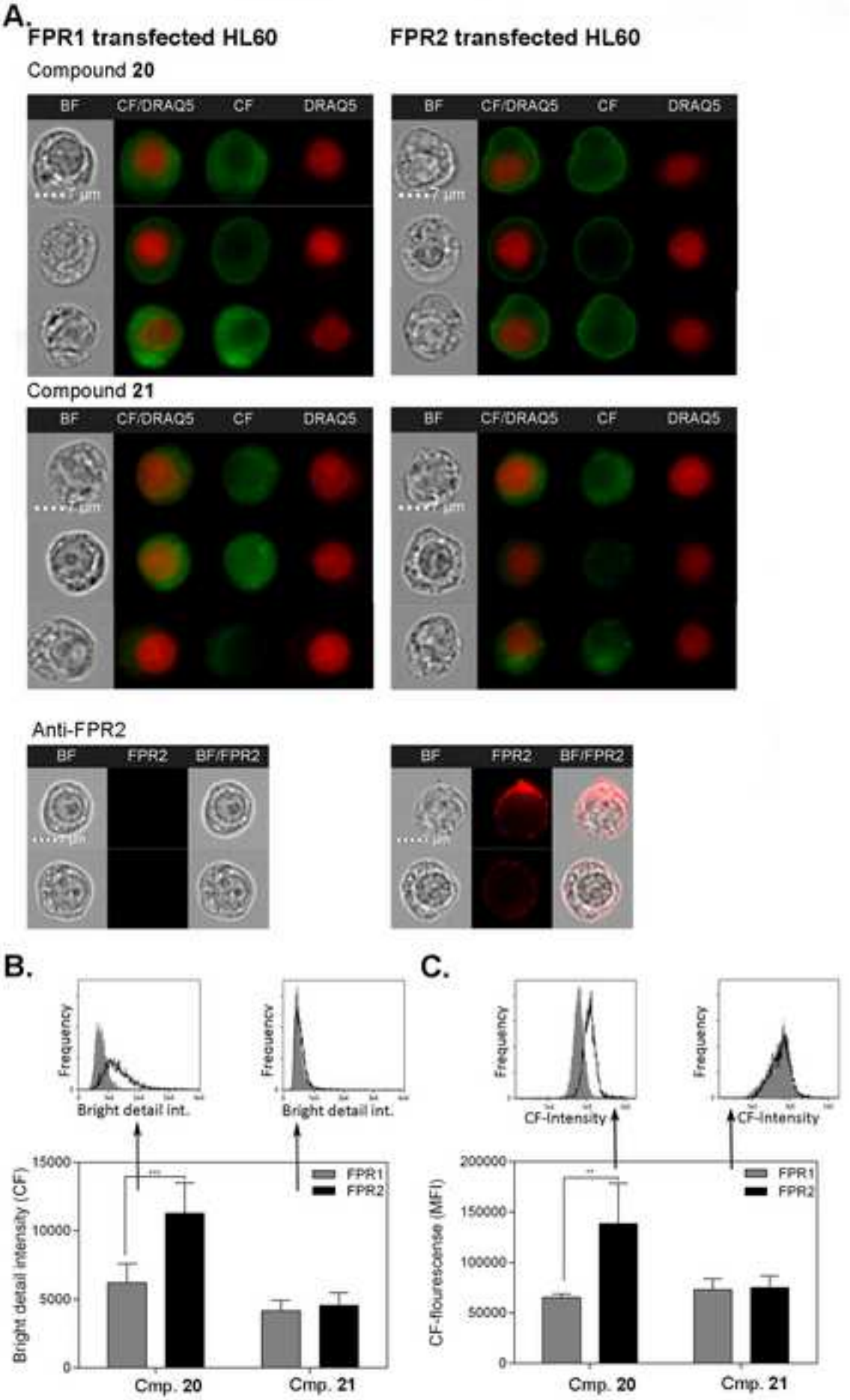

**Figure 8**

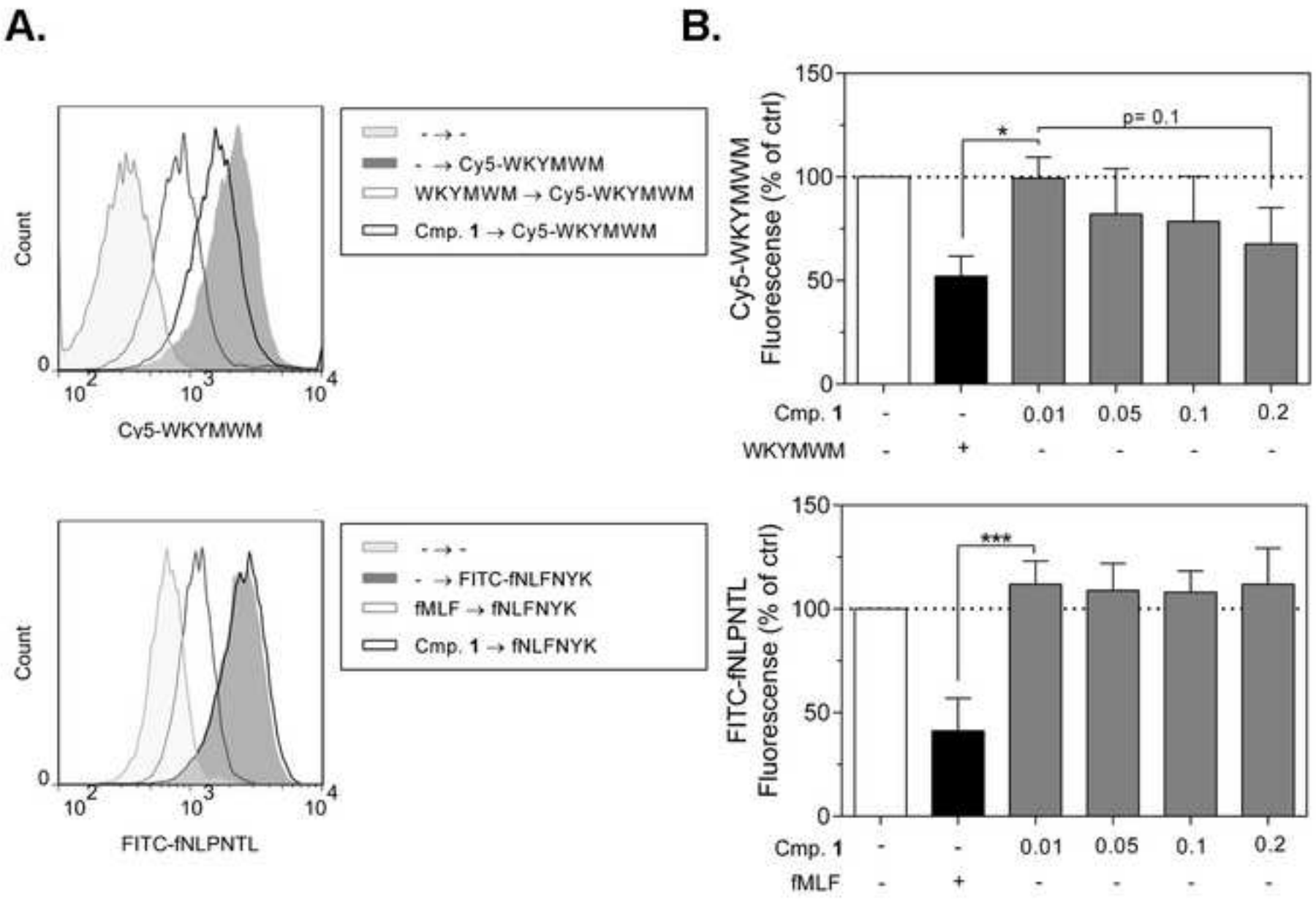
A.
Count
0
$10^2$
$10^3$
$10^4$
Cy5-WKYMWM
- → -
- → Cy5-WKYMWM
WKYMWM → Cy5-WKYMWM
Cmp. 1 → Cy5-WKYMWM
Count
0
$10^2$
$10^3$
$10^4$
FITC-fNLPNTL
- → -
- → FITC-fNLFNYK
fMLF → fNLFNYK
Cmp. 1 → fNLFNYK
B.
Cy5-WKYMWM Fluorescense (% of ctrl)
150
100
50
0
*
p= 0.1
Cmp. 1 - - 0.01 0.05 0.1 0.2
WKYMWM - + - - - -
FITC-fNLPNTL Fluorescense (% of ctrl)
150
100
50
0
***
Cmp. 1 - - 0.01 0.05 0.1 0.2
fMLF - + - - - -